PROJECT

Turbulence beneath the free surface

Technical Report

Experiments on turbulence beneath the free surface generated by an airfoil

Hydraulics Laboratory, DICATeA, University of Parma, Italy

July 2011

Francisco M. Domínguez*, Luca Chiapponi**, María José Polo*, Sandro Longo**

***Grupo de Investigación de Dinámica Fluvial e Hidrología**

Universidad de Córdoba, Spain

**** Dipartimento di Ingegneria Civile, dell'Ambiente, Territorio e Architettura**

Università degli Studi di Parma, Italy

This report is the result of the experimental activity carried out by the authors in the Laboratory of Hydraulics, Department of Civil Engineering, University of Parma, during the short stay of Francisco Domínguez Luque as Ph.D student from the University of Cordoba under mobility from the beginning of May to the end of July 2011.

The collaboration was programmed inside the Cooperation Protocol between the University of Parma and the University of Cordoba, with Sandro Longo responsible for the italian part and Maria Jose Polo Gomez responsible for the spanish part.

Parma, Cordoba, September 2011

The Authors

final revision in May 2012

INDEX

1. INTRODUCTION

An understanding of the structure and dynamics of free-surface turbulence is essential for the correct interpretation of many interface phenomena, and the need for measuring turbulence characteristics beneath a free surface arises from its role in many important phenomena taking place at interfaces, such as gas and heat exchange in the ocean, which have huge influences on the balance of chemicals and energy. In many engineering and industrial problems, most exchange takes place at the interface between a gas and a fluid, and many large-scale physical problems are governed by turbulence characteristics beneath an interface.

The free surface represents a boundary for the flow domain and imposes some conditions: the material derivative of the free surface must be zero, while the tangential stresses should be zero unless a shear is exerted by the overflowing gas. The interaction between turbulence and a free surface is expected to vary with the level of turbulence. The two main measures for describing the phenomenon are the Reynolds number and the Froude number, which generally increase as a pair. At reduced Froude numbers, a free surface is essentially unaffected by the turbulence of the flow beneath, is almost flat and imposes only a reduction in the normal velocity component. In this limit, it can be described as a slip-free rigid flat surface. At higher Froude numbers, the free surface is not flat, and an energy exchange with the fluid flow starts. Such an exchange is assumed to be initially very limited, but to be quite strong for a free surface which loses its connectivity and includes air bubbles and drops. There are a great variety of free surface patterns and several mechanisms of energy transfer at a free surface such as capillary and gravity waves.

Many different ways to generate turbulence in the water side impinging the interface from below have been adopted and are documented in literature. The present experiments make use of an airofoil in water able to generate a wake partially reaching the free surface from the water side.

The aim of this report is to detail all the methods, techniques, solutions to practical problems encountered during the experiments and to give all the information necessary for post processing the acquired data.

2. EXPERIMENTAL FACILITIES AND EXPERIMENTS

The experiments were conducted in the flume in the Laboratory of Hydraulics of the Department of Civil Engineering, Environment, Planning and Architecture (DICATeA) of the University of Parma, Italy. The flume is 0.30 m wide, 0.45 m high and 10 m long, the sidewalls are made of glass, the bottom is in stainless steel. A flow straightener at the entrance eliminates the large scale vortices and eddies. A bottom hinged flap gate at the downstream end of the flume allows water level control.

Figure 1. Bottom hinged flap gate (left) and the flow straightener in the flume (right)

The inclination of the bottom can be made positive or negative, with an electro mechanic actuator. To circulate the water stored in three tanks, there is a centrifugal pump and a PID regulator controlling an electric valve that diverts part of the flow and guarantees the stability of the desired flow rate in the flume. The flow rate is measured by a Promag Hendress-Hauser magflow, with an accuracy of 0.5% of the instantaneous measured value. The maximum flow rate is ≈ 28 l/s. The water used in the experiments is tap water seeded with clay, to facilitate the subsequent acquisition of information with some of the instruments used for velocity measurements.

Figure 2. Overview of the flume and of the pump, with the PID system active

The experiments were conducted in July 2011, within external environmental conditions typical of a parmesan summer, maximum and minimum average temperatures between 29 and 18 degrees Celsius and relative humidity values close to 60%. The internal conditions were not so different from the external one.

The purpose of the present study is the analysis of turbulence induced by an airfoil beneath the water free surface, its interaction with free surface oscillations, with special reference to the model proposed by

Peregrine and Svendsen (1978) for the flow field in a class of steady or quasi-steady breakers (Battjes and Sakai, 1981). The main scheme is similar to the one adopted by Battjes and Sakai, 1981, with some modifications. A 6024 NACA airfoil was planned and built up with a support structure in Aluminium that interfered minimally in the circulating flow and allowed the airfoil to be moved upstream and downstream along the flume and to vary the inclination with respect to the horizontal. The frame is fixed to a trolley which can be moved on two railways on the top of the flume. The cord length of the profile is c = 100 mm.

Figure 3. Section of measurements with the NACA 6024 airfoil in place, the mirror at the bottom for reflecting the light sheet, the dark surface fixed on the glass wall opposite to the PIV to minimize reflections

Velocity measurements were carried out with a particle image velocimeter (PIV), which provided information in 2D along the longitudinal section of the flume. In addition to the horizontal and vertical velocity, also vorticity, Turbulent Kinetic Energy (TKE), Reynolds stresses and intermittency factor could be computed. A calibration step was carried out for an Ultrasound doppler velocity profiler (UDVP), able to measure the three velocity components along an axis. Finally an ultrasonic water level sensor (US) was used to measure water level fluctuations.

Figure 4. Laser and camera for the PIV (left), and UDVP placed on the bottom (right)

The following sections describe with more detail each of the tools and elements that take part on the system settled for the study of turbulence. If some extra information about the instruments is needed, some reinforcement lectures are Chiapponi L. et al (2010) (Experiments carried out in wind tunnel II) and the Operations Manual of the PIV.

NACA 6024 AIRFOIL

The breaker introduced in the flume was an airfoil NACA (National Advisory Committee on Aeronautics) Four-Digit Series 6024. This airfoil belongs to the family of airfoils designed using the methodology published in *The Characteristics of 78 Related Airfoil Sections from Tests in the Variable Density Wind Tunnel.* The first digit specifies the maximum camber (m) in percentage of the chord (airfoil length), the second indicates the position of the maximum camber (p) in tenths of the chord, and the last two numbers provide the maximum thickness (t) of the airfoil in percentage of chord. Using these m, p and t values, the coordinates for the entire airfoil can be computed using the relationships attached in APPENDIX 1. The profile was made in Polymethyl methacrylate (PMMA) with a milling machine CNC. The cord length is c = 100 mm.

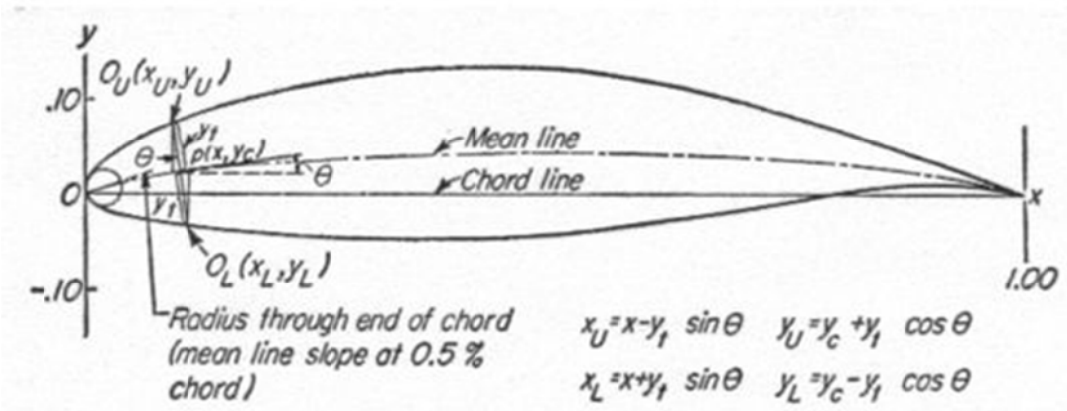

Figure 5. NACA airfoil geometrical construction

ULTRASONIC DOPPLER VELOCITY PROFILER (UDVP)

As part of the present experiments, there was also the calibration of the UDVP. The instrument is manifactured by Signal Processing, Switzerland, model DOP2000, 2005, and the carrier frequency of the probes was 8 MHz (TR0805LS) (the arrangement of the probes is shown in Fig. 1*e*). The transducers had active element diameters of 5 mm in an 8 mm (diameter) cylindrical plastic housing. The arrangement of the probes was chosen to guarantee an overlap of the measurement volume in the area of interest.

Each transducer measured the axial velocity component as a function of the axial position. The velocity profile was measured in several tens of spatial positions (gates), starting from 3 mm in front of the probe head, and was assumed to be in the centre of the measuring volumes. The measuring volume of a single gate was approximately disk-shaped, with a thickness related to the operating condition and a diameter that was almost invariant (nominally equal to 5 mm in the near field zone, ~33 mm long for the probe used in water). The measuring volume increased in the far field progressively due to lateral spreading of the US energy, with a half diverging angle of 1.2° for the probe used in water. The actual diameter of the measuring volume is smaller than the nominal volume if the correct sensitivity level and beam power are selected. In fact, a reduced sensitivity during the echo reception (i.e., a high level of energy of the echoes requested to process the signal) and a high power of the US beam favour the backscatter of the particles near the axis of the beam (the US power decreases in the radial direction as well as the axial direction) and thus focus the volume of measurements in the near-axis region. Balancing this, multiple particles or micro-eddies present in the volume of measurement scatter the echoes and broaden the spectral peak, whereas diffraction tends to enlarge the measurement volume. The thickness of the sampling volumes is assumed to be equal to half the wavelengths contained in a burst, unless the electronic bandwidth of the instrument is limiting. In our experimental setup, this last variable is the limiting factor that determines the minimum thickness of the sampling volume (0.68 mm in water). The overall size of the measurement volumes allows only the detection and analysis of macroturbulence, but this limitation is outweighed by some advantages, such as the large number of measurement points that are almost simultaneously available. In addition, the larger size of the measurement volumes is in the horizontal plane, and, in the flow field of the present experiments, the fluid velocity has a moderate spatial gradient in the horizontal direction. The most important spatial gradient is expected in the vertical dimension, and the resolution in the vertical axis is comparable to the resolution obtained using Laser Doppler Anemometry, Particle Image Velocimetry or Thermal Anemometry. The distance between two gates varied in different tests from 0.72 to 0.95 mm, as measured along the beam axis using non-overlapping measurement volumes. Each profile is obtained as an average of a multiple set of emissions (4, 8, 16, etc.) of a burst containing multiple waves (2, 4, 8, etc.). The

acquisition is multiplexed with circular scanning of a single profile for each probe. The time lag between two different probe measurements depends on the general configuration and can be of the order of ~ 0.03 s on average, whereas the time lag of the pulse from one gate to another is $k\delta z/c$, where k is a coefficient (~2), δz is the distance between two gates and c is the ultrasound celerity in water. The velocity resolution is 1/128 (1 Least Significant Bit) of the velocity range (~0.8% FS). For all tests, this was better than 4 mm/s (the velocity measured along the probe axis).

There are some effects to be considered in evaluating the reliability of the measurements made using UDVP. The presence of the moving interface generates a Doppler shift that is highly energetic and can persist in the flow field as a stationary signal. The elimination of these stationary components by high-pass filtering implies an increase in the dynamic of the analysed echoes and a reduction in the sensitivity of low velocity measurements. Unfortunately, the Doppler frequency shift induced by these mobile interfaces cannot be removed if its value is the same as that of the flowing particles. To balance all these effects, the presence of some artifacts is tolerated.

The main sources of uncertainty for the UDVP are Doppler noise, the presence of air bubbles or highly reflective interfaces, and the gradient of temperature in the liquid medium.

Doppler noise is essentially a Gaussian white noise and depends on the seeding particles and on the presence of gas bubbles. The effects of gas bubbles are quite dramatic: even though the celerity of the Ultrasound carrier is essentially not affected if the bubble void fraction is < 0.1, the UDVP system measures the bubbles' velocities, and these can be much different from the fluid velocity if the bubbles are large. In the presence of bubbles or highly reflective interfaces, several velocity spikes are recorded that are not due to turbulence.

The uncertainty in the position of the gates and in the fluid velocity evaluation is due to the mean celerity of the Ultrasounds, which is affected by the temperature and density of the fluid. Considering pure water and assuming that the temperature varies linearly between the emitter and the gate, the relative uncertainty in the position of the gate is equal to:

$$\frac{\Delta L}{L_0} = \frac{c_1^2 - c_0^2}{4c_0^2}.$$

Here, L_0 is the distance of the gate from the emitter/receiver as measured at the nominal uniform celerity c_0 (the celerity near the emitter/receiver with a fluid temperature Θ_0) and c_1 is the celerity near the gate with a local fluid temperature equal to Θ_1. The uncertainty in travel time measurements has been neglected because the electronics allow for very accurate estimations of the interval time. Assuming $\Theta_0 = 288$ °K and $\Theta_1 = \Theta_0 \pm 1$ °K, then $c_0 = 1462.8$ m/s, $c_1 = 1462.8 \pm 2.7$ m/s, the relative uncertainty $\Delta L/L_0 = 0.1\%$ and the absolute uncertainty = ± 0.1 mm at a distance of 100 mm.

The evaluation of the uncertainty in fluid velocity evaluation requires a short description of the principle of the Ultrasonic Doppler Velocity Profiler that we used. In the UDVP adopted, the emitter periodically sends a short ultrasonic burst (four waves per burst in the setup used), and a receiver (coincident with the emitter) collects echo issues from targets that may be present in the path of the ultrasonic beam. By sampling the incoming echoes at the same time relative to the emission of the bursts, the displacements of scatters along the beam axis are detected, and from these, the fluid velocity along the beam axis (assumed equal to the velocity of the scatters) is computed as:

$$u = \frac{c(t_2 - t_1)}{2t_{prf}},$$

where t_{prf} is the time between two subsequent pulses, t_1 is the travel time of the first pulse and t_2 is the travel time of the second pulse. Assuming that the two events, "travel of the first pulse" and "travel of the second pulse", are not correlated, the absolute uncertainty in the velocity estimation can be computed as:

$$\Delta u = \frac{L_0}{2t_{prf}} \frac{\Delta(L_2 - L_1)}{L_0} = \frac{L_0}{t_{prf}} \frac{\Delta L}{L_0}.$$

This is very large for most of the operating conditions (e.g., setting $t_{prf} = 3\times10^{-4}$ s for measurements in a gate at L_0 = 100 mm and assuming $\Delta L/L_0$ = 0.1% results in Δu = 0.33 m/s). In practical situations, if turbulence in the flow field has a time scale larger than t_{prf}, the fluctuations of celerity along the path have a similar pattern for the two subsequent pulses and this results in $\Delta(L_2 - L_1) << 2\Delta L$. In addition, the velocity is estimated as the average of several bursts, with a consequent reduction in the uncertainty.

A last source of uncertainty arises from the finite size of the measurement volumes, which affects the velocity measurements and the Reynolds stress estimates. Here, this uncertainty is negligible with respect to the other sources of uncertainty.

The overall accuracy in the velocity measurements under carefully controlled conditions can be assessed as 3% of the instantaneous value, with a minimum equal to 0.8% of the Full Scale (less than 4 mm/s for most tests).

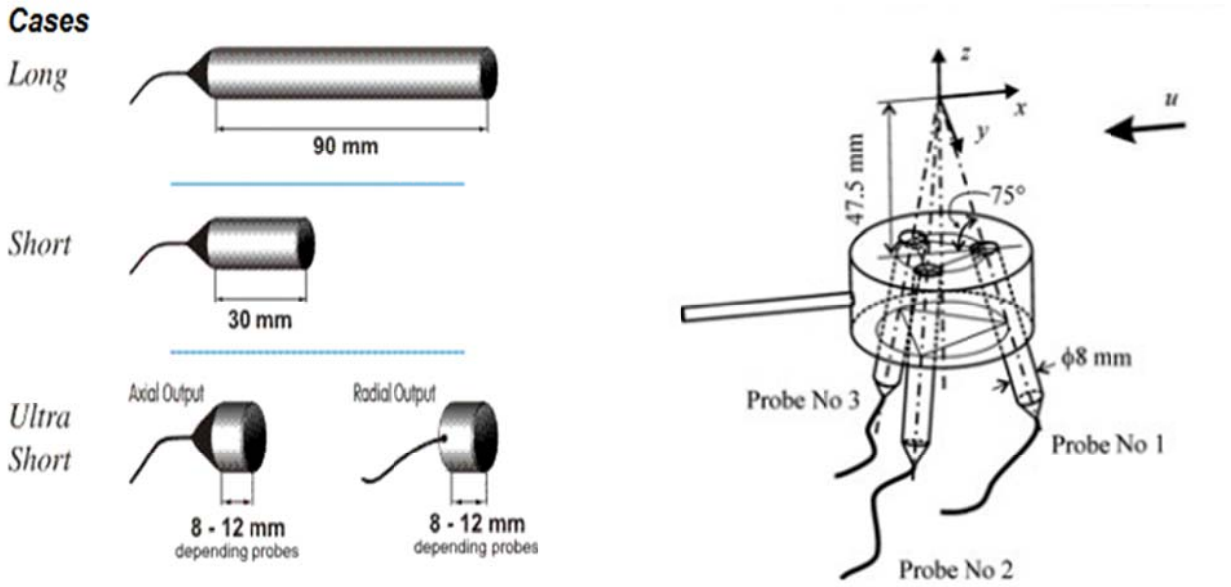

Figure 6. Ultrasonic transducers. Scheme of the probe.

The four transducers were placed in a structure to fix them in the flume, as it can be seen in Figure 7. The angle of the beam with respect to the horizontal was 75 grades for probes 1, 2 and 3 and 90 grades for probe 4, so that a Matlab routine was needed to change the data in axis "1", "2" and "3" (axis of the beam of each probe) to data in the axis "x", "y" and "z". The routine is attached in APPENDIX 2 (note that probe 4 was added later, in the final disposition observed in Figure 8, so a small change in the routine can be done to use probe 4 to improve the measurement in the vertical axis).

Figure 7. Disposition of the transducers. View from side and above.

The monitor enables users to change parameters, to view the evolution of the velocity profile and record it, and to use the trigger or the multiplexer mode. In this study, the mode used was multiplexer, so that the three probes could be used. In the multiplexer mode the software enables acquisition procedures based on defined numbers of profiles acquired from each transducer connected to the multiplexer.

Calibration of the UDVP

The calibration of the UDVP was initially performed with a single probe and by using the PIV for comparison, which is intrinsecally more accurate and precise than the UDVP. The single probe was placed in the middle of the flume from above, as can be seen on Figure 8.

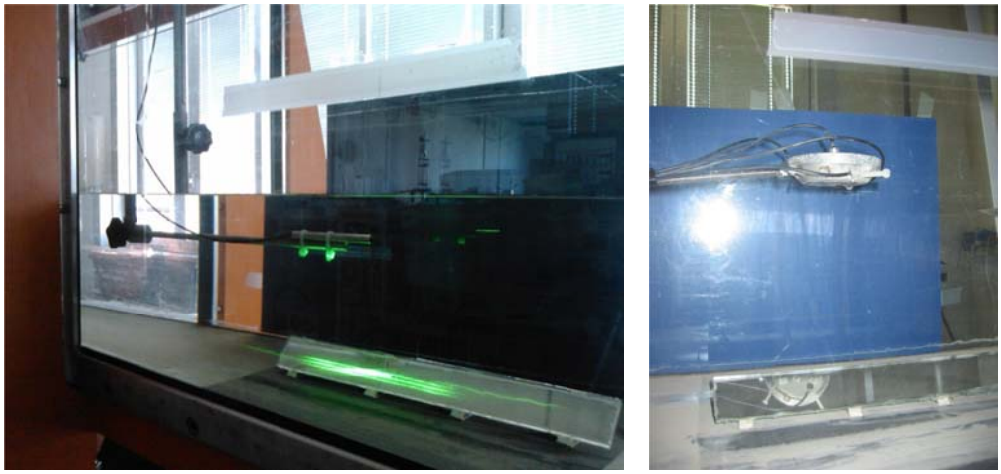

Figure 8. Single probe (left) and multi-probe (right) in the configuration adopted for calibration of the UDVP. The green light of the laser emission is visible

In a second step also the calibration of the multiprobes was performed.

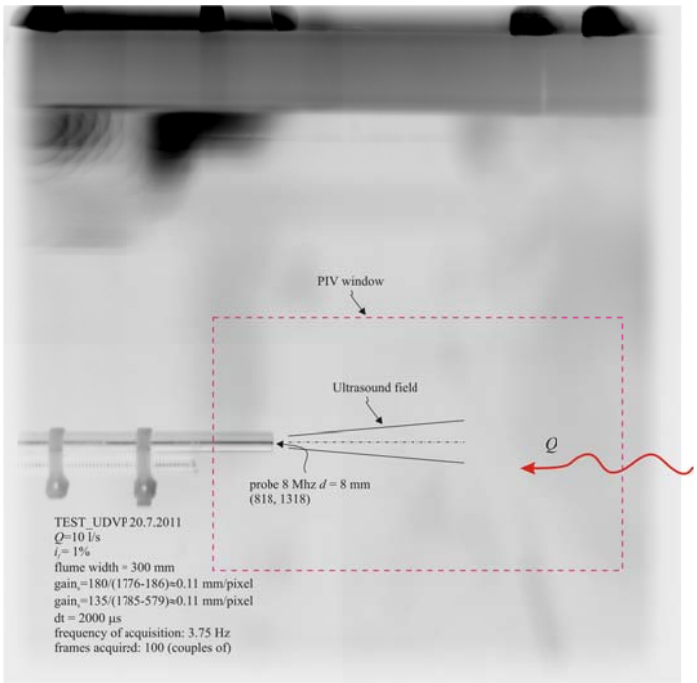

Figure 8bis. Single probe test calibration for PIV acquisition

The calibration required the following steps:

- The single probe was aligned with the laser sheet reflected by the mirror, as can be seen in Figure 8.
- In the computer for the PIV, the folder UDVP_calibration was created, and some captures were stored (in this case, 10 captures were stored). These images needed to be validated.
- In the dedicated computer for the UDPV, where the single probe that is pointing to the airfoil is connected, the velocity profile, in the axis that is pointing to the airfoil, can be seen in real time and stored. As can be observed in Figure 9, the profile is not uniform near the probe head due to the probe disturbances.

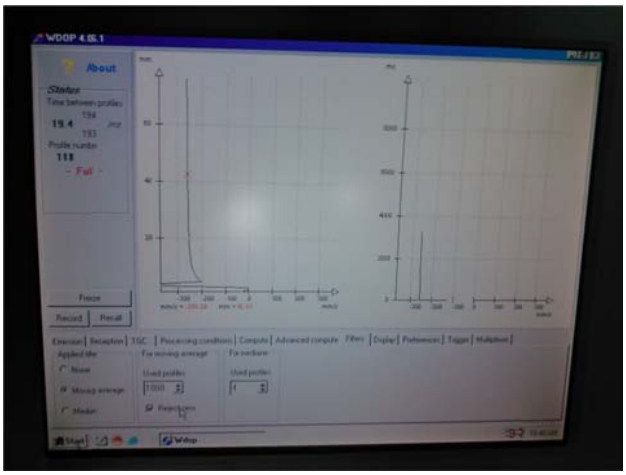

Figure 9. Real time monitor velocity profile along the axis of the single probe

- To water discharge was fixed in 10.00 ± 0.1 l/s and with initial water temperature of 23.58 °C at 11:05 a.m. with ρ_w =997.5 Kg/m^3, ε = 2.195 × 10^9 Pa, c = (ε / ρ_w)$^{1/2}$ = 1.483 m/s. This last value needs to be inserted as parameter in the UDPV or can be used for correcting the data during post processing.
- In the computer for the UDPV the archive test_UDPV_PIV_1 was created to store the data measured with the UDPV and compare with the data acquired with the PIV. 10 000 profiles were recorded in 187.32 seconds.
- At the same time 100 frames were recorded in the test named test_UDPV_PIV_1 with the PIV and stored in the folder named francisco_UDPV_vs_PIV.
- A second data acquisition for this flow rate was done with the UDPV and the PIV. This second data acquisition was done for check.
- The repetition of the steps given for 15.00 ± 0.1 l/s was done with a water temperature of 23.88 °C at 11:34 AM.

- The repetition of the steps given for 20.00 ± 0.1 l/s was done with a water temperature of 24.08 °C at 11:50 AM in the morning. (Last test with the UDPV was named test_UDPV_PIV_6).

For a calibration with limited turbulence level, two of this runs were repeated removing the airfoil from the flume. Repetitions were carried out during the afternoon same day. Steps given to obtain data for calibration were the following:

- First take out the airfoil from the flume and measure water temperature (at 6:52 PM it was 24.02 °C)
- Proceed the same way as it was done for the runs in the morning (c =1.483 m/s).
- This time 700 frames were recorded with the PIV and during the PIV was acquiring data two archives were recorded with the UDPV. First, 10 000 profiles and 128 emissions per profile (the same as the acquisitions in the morning). Second, 40 000 profiles and 16 emissions per profile.

These steps were done twice, for a 20.00 ± 0.1 l/s flow rate and for a 10.00 ± 0.1 l/s flow rate.

Table 1. Data for UDPV calibration runs

Flow rate (l/s)	**Time (24 hr)**	**Water Temp (°C)**	**UDPV profiles**	**UDPV *epp**	**PIV images**	**Directory in the folder francisco_UDPV_vs_PIV**
10	11:05	23.58	10000	128	100	test_UDPV_PIV_1
10			10000	128	100	test_UDPV_PIV_2
15	11:34	23.88	10000	128	100	test_UDPV_PIV_3
15			10000	128	100	test_UDPV_PIV_4
20	11:50	24.08	10000	128	100	test_UDPV_PIV_5
20			10000	128	100	test_UDPV_PIV_6
20	18:52	24.02	10000	128	700	test_UDPV_PIV_7
20			40000	16	700	test_UDPV_PIV_8
10			10000	128	700	test_UDPV_PIV_9
10			40000	16	700	test_UDPV_PIV_10

*epp (emissions per profile)

After post processing the data, some results were elaborated and are shown in the following Figures.

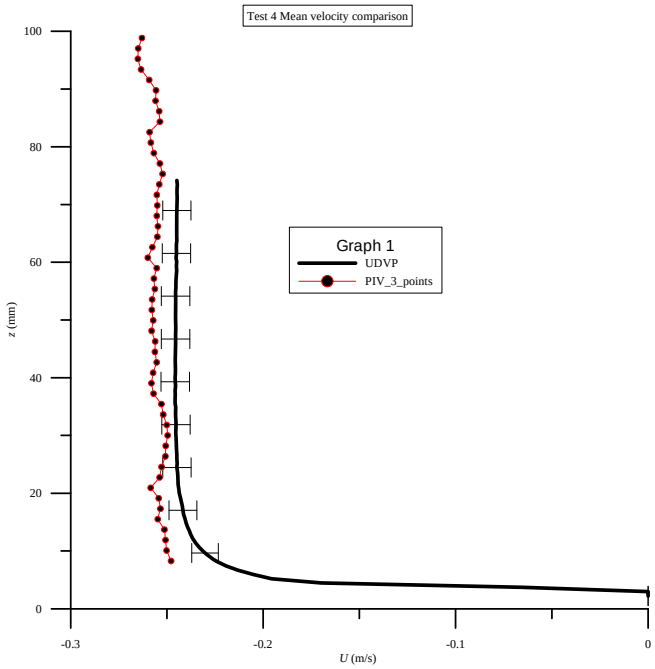

Figure 10. Mean velocity, Test 4, Q = 15 l/s, hydrofoil present. UDVP: 10 000 profiles data rate ≈ 50 Hz, 128 emissions per profile; PIV: 100 frames, data rate 3.75 Hz. Error bar ± 3%. Sound celerity: 1483 m/s at T = 23.5 °C

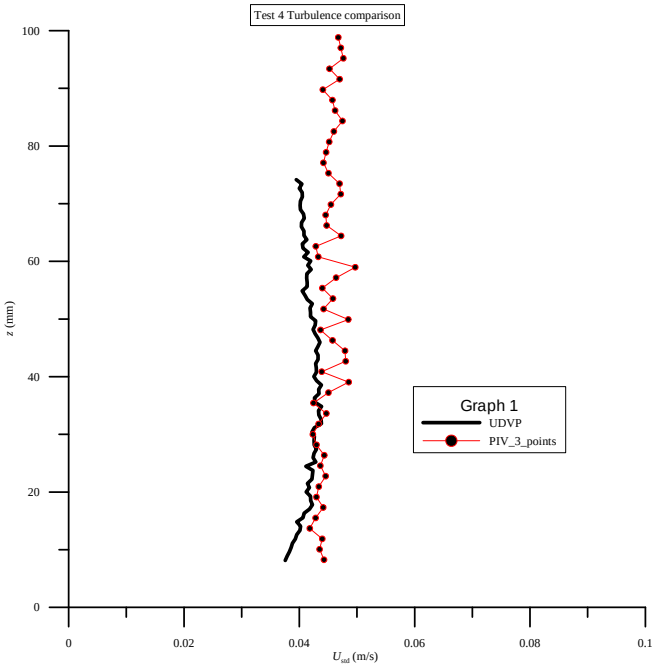

Figure 11. Turbulence, Test 4, Q = 15 l/s, hydrofoil present. UDVP: 10 000 profiles data rate ≈ 50 Hz, 128 emissions per profile; PIV: 100 frames, data rate 3.75 Hz. Sound celerity: 1483 m/s at T = 23.5 °C

In this case UDPV measurements were improved using the data for the 10 000 profiles. First time the data for 100 profiles were used and the graphic was more coarse.

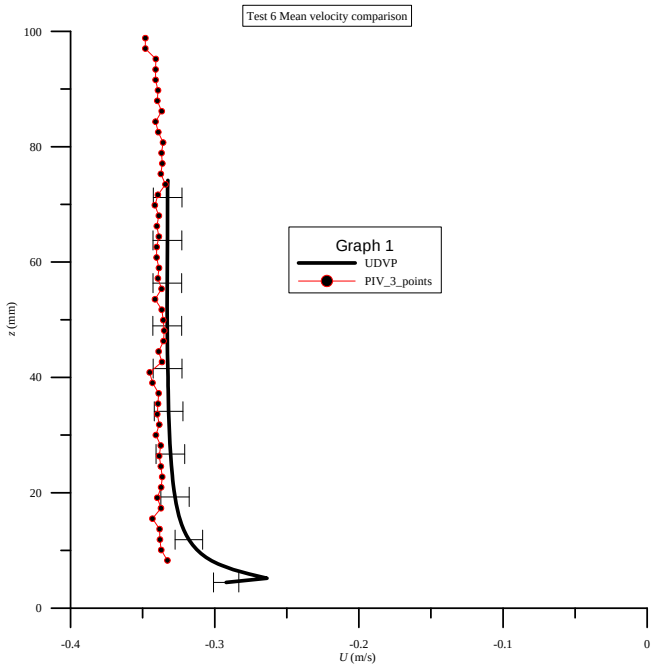

Figure 12. Mean velocity, Test 6, Q = 20 l/s, hydrofoil present. UDVP: 10 000 profiles data rate ≈ 50 Hz, 128 emissions per profile; PIV: 100 frames, data rate 3.75 Hz. Error bar ± 3%. Sound celerity: 1483 m/s at T = 23.5 °C

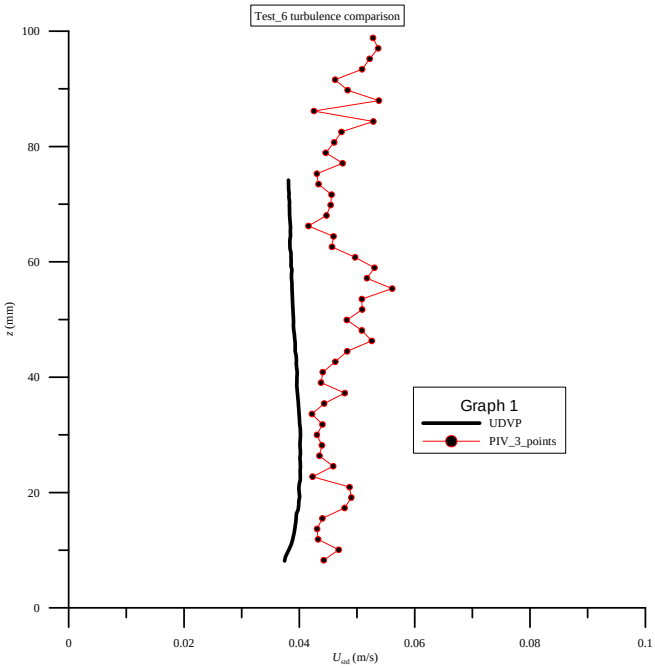

Figure 13. Turbulence, Test 6, Q = 20 l/s, hydrofoil present. UDVP: 10 000 profiles data rate ≈ 50 Hz, 128 emissions per profile; PIV: 100 frames, data rate 3.75 Hz. Sound celerity: 1483 m/s at T = 23.5 °C

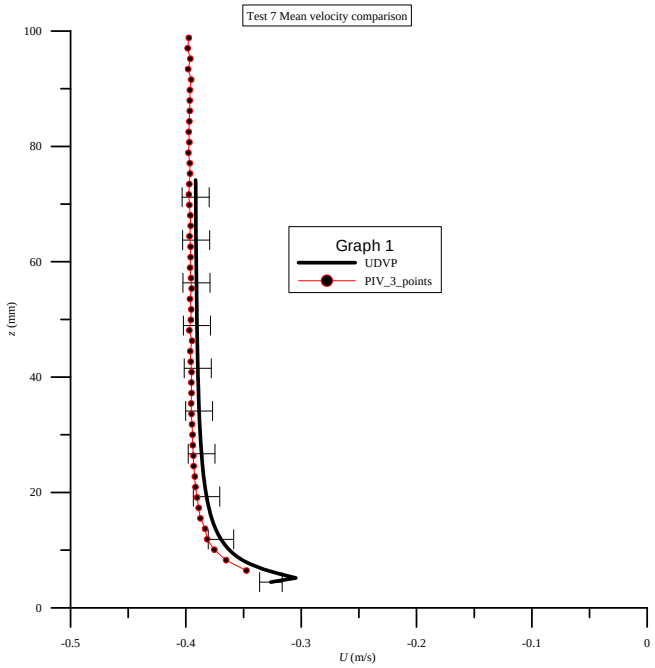

Figure 14. Mean velocity, Test 7, Q = 20 l/s, hydrofoil absent. UDVP: 40 000 profiles data rate ≈ 50 Hz, 128 emissions per profile, 128 emissions per profile; PIV: 700 frames, data rate 3.75 Hz. Error bar ± 3%. Sound celerity: 1483 m/s at T = 23.5 °C

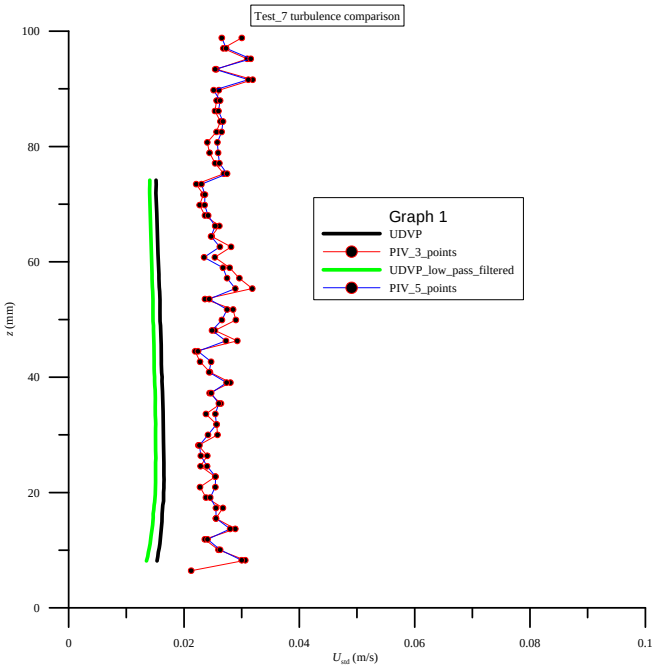

Figure 15. Turbulence, Test 7, Q = 20 l/s, hydrofoil absent. UDVP: 10 000 profiles data rate, ≈ 50 Hz, 128 emissions per profile; PIV: 700 frames, data rate 3.75 Hz. Sound celerity: 1483 m/s at T = 23.5 °C. Black line: UDVP; green line: UDVP low pass filtered at 3.75 Hz

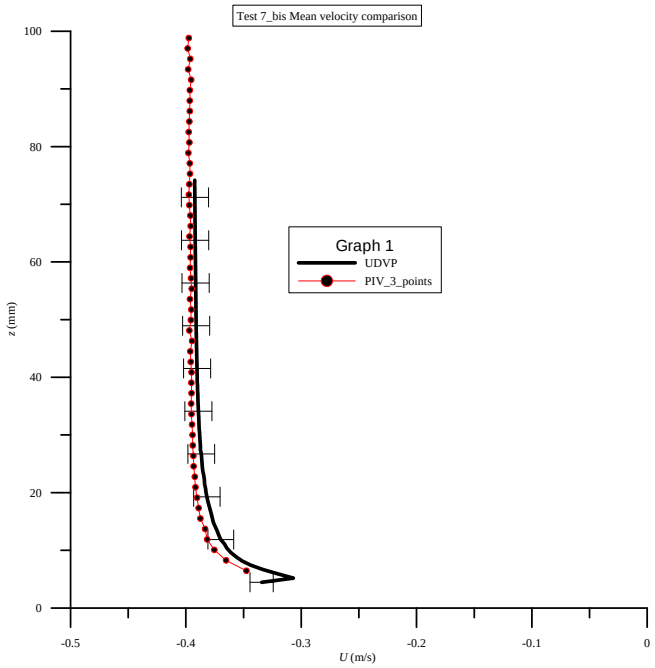

Figure 16. Mean velocity, Test 7_bis, Q = 20 l/s, hydrofoil absent. UDVP: 40 000 profiles data rate ≈ 200 Hz, 16 emissions per profile; PIV: 700 frames, data rate 3.75 Hz. Error bar ± 3%. Sound celerity: 1483 m/s at T = 23.5 °C

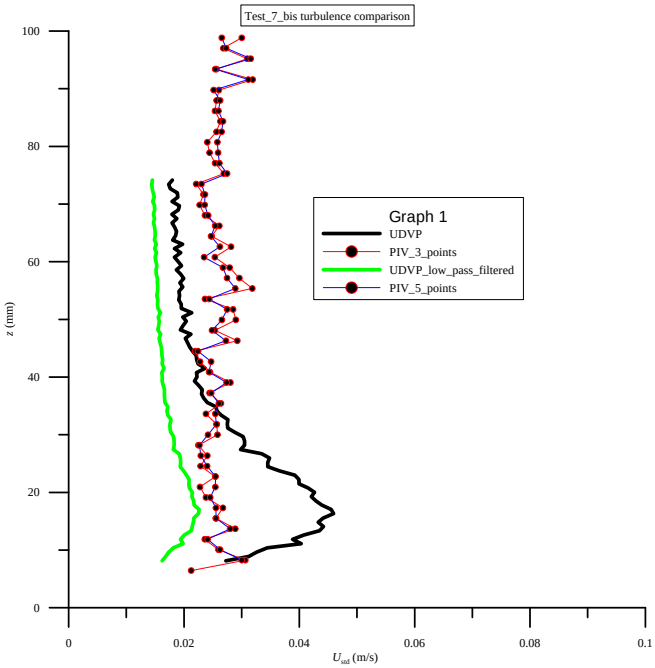

Figure 17. Turbulence, Test 7_bis, Q = 20 l/s, hydrofoil absent. UDVP: 40 000 profiles data rate, ≈ 200 Hz, 16 emissions per profile; PIV: 700 frames, data rate 3.75 Hz. Sound celerity: 1483 m/s at T = 23.5 °C. Black line: UDVP; green line: UDVP low pass filtered at 3.75 Hz

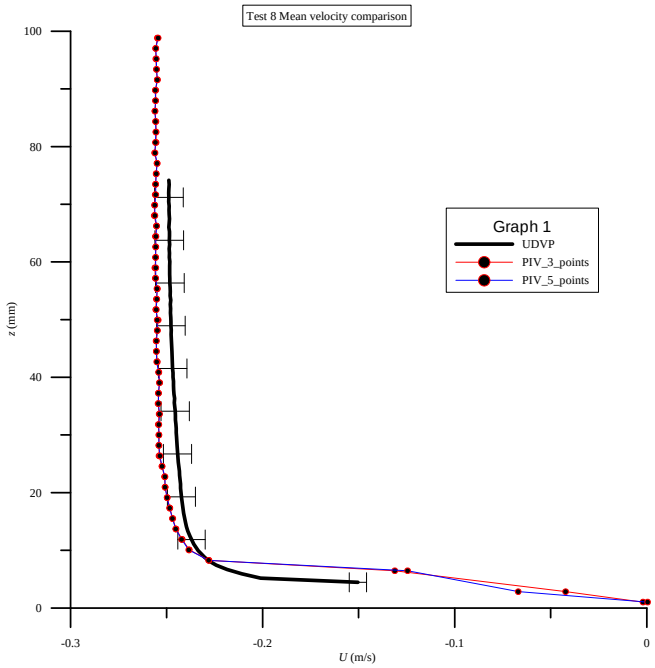

Figure 18. Mean velocity, Test 8, Q = 10 l/s, hydrofoil absent. UDVP: 10 000 profiles data rate ≈ 50 Hz, 128 emissions per profile; PIV: 700 frames, data rate 3.75 Hz. Error bar ± 3%. Sound celerity: 1483 m/s at T = 23.5 °C

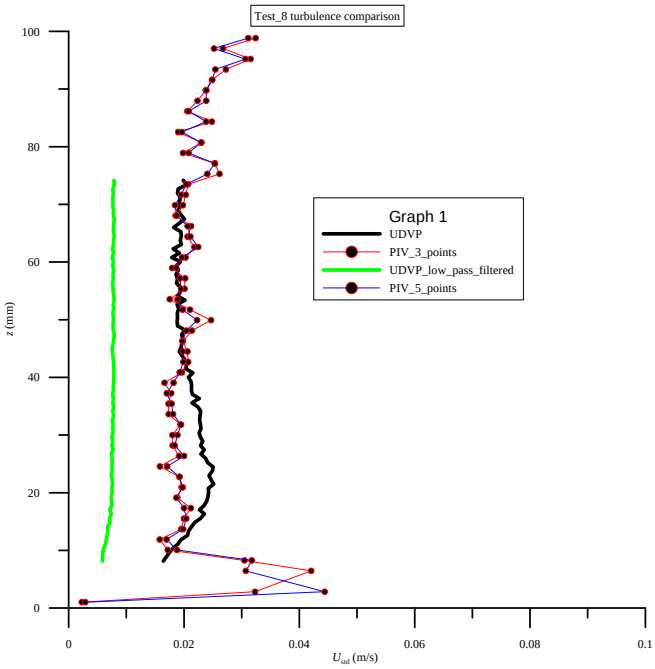

Figure 19. Turbulence, Test 8, Q = 10 l/s, hydrofoil absent. UDVP: 40 000 profiles data rate, ≈ 50 Hz, 128 emissions per profile; PIV: 700 frames, data rate 3.75 Hz. Sound celerity: 1483 m/s at T = 23.5 °C. Black line: UDVP; green line: UDVP low pass filtered at 3.75 Hz

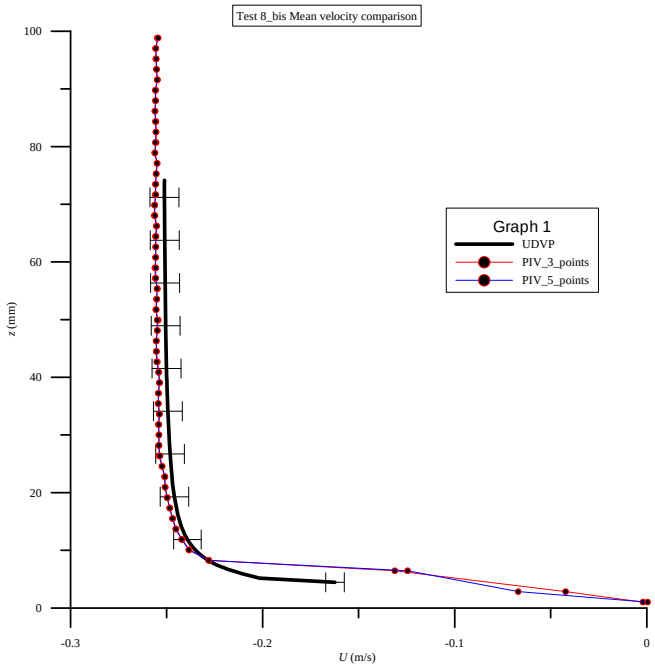

Figure 20. Mean velocity, Test 8_bis, Q = 10 l/s, hydrofoil absent. UDVP: 40 000 profiles data rate ≈ 200 Hz, 16 emissions per profile; PIV: 700 frames, data rate 3.75 Hz. Error bar ± 3%. Sound celerity: 1483 m/s at T = 23.5 °C

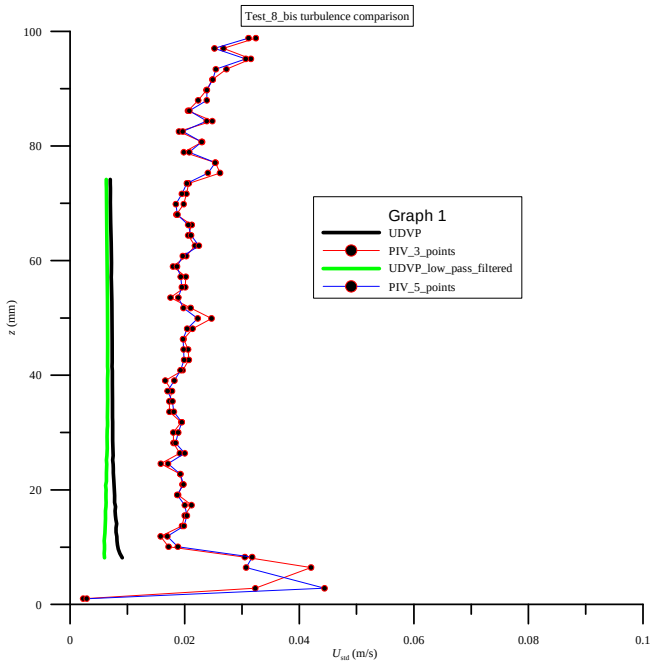

Figure 21. Turbulence, Test 8_bis, Q = 10 l/s, hydrofoil absent. UDVP: 40 000 profiles data rate, ≈ 50 Hz, 128 emissions per profile; PIV: 700 frames, data rate 3.75 Hz. Sound celerity: 1483 m/s at T = 23.5 °C. Black line: UDVP; green line: UDVP low pass filtered at 3.75 Hz

Some indications arise after calibration. First that is not necessary to use low pass filter, UDPV and PIV measurements are more similar without it; and second that there is not much difference between data with 5 and 3 points using the PIV.

After this calibration, other tests were done to calibrate the multiprobes tool (Figure 7) with the fourth probe installed. The multiprobes tool was placed using the same supporting structure used for the single probe, see Figure 8 but the probes where pointing to the bottom of the flume, also to the mirror, so that the laser sheet would coincide with the centre of the multi-probes tool.

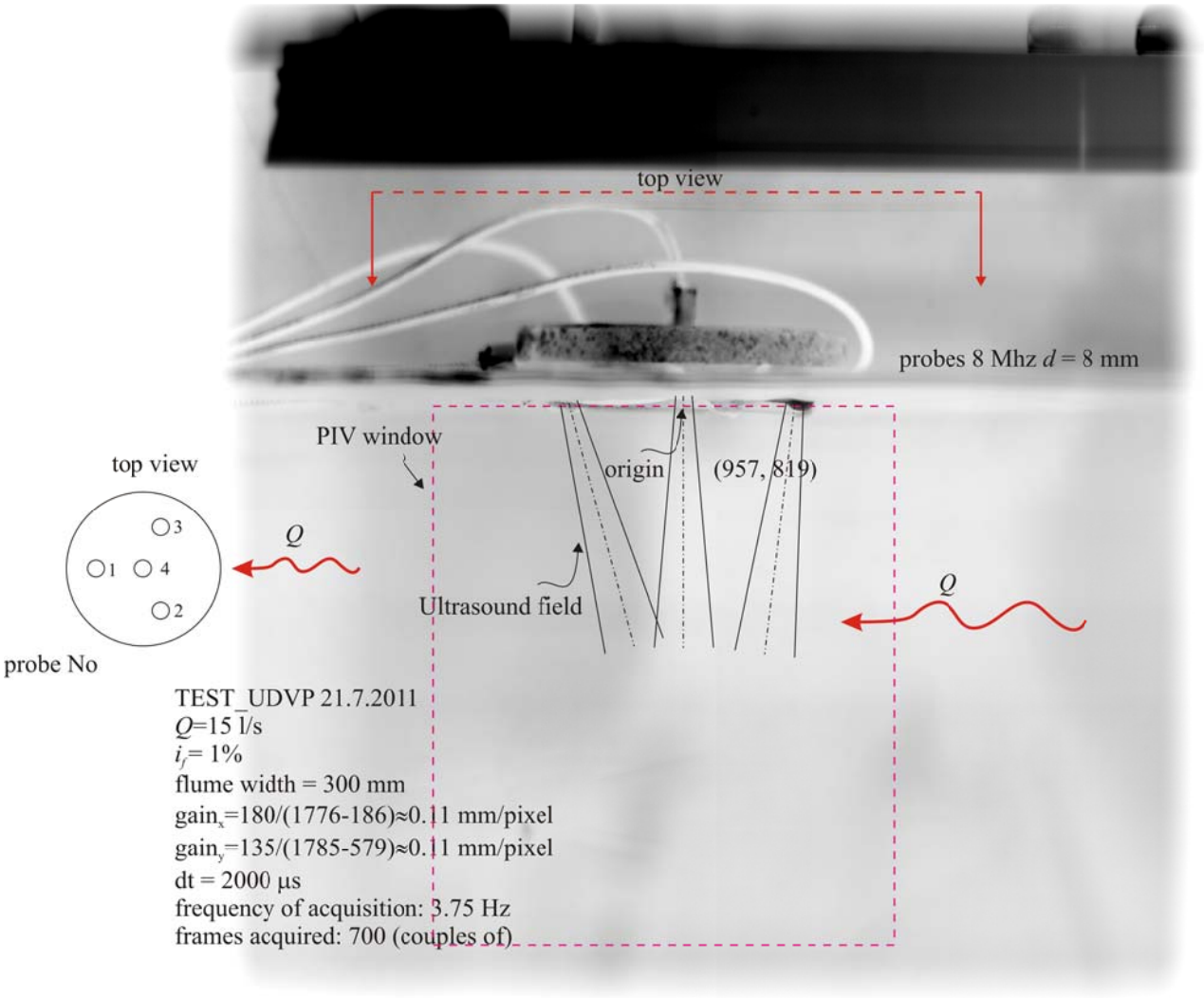

Figure 22. Reference system for the 4 UDVP calibration

The data referred to these last tests have not been yet analysed.

PARTICLE IMAGE VELOCIMETER

Particle image velocimetry (PIV) is an optical method of flow visualization and measurement used in research. It is used to obtain instantaneous velocity measurements and related properties in fluids. The fluid is seeded with tracer particles which, for sufficiently small particles, are assumed to follow the flow dynamics. The fluid with entrained particles is illuminated so that particles are visible. The motion of the seeding particles is used to calculate speed and direction (the velocity field) of the flow being studied.

Other techniques used to measure flows are Laser Doppler velocimetry and Hot-wire anemometry. The main difference between PIV and those techniques is that PIV produces two dimensional or even three dimensional vector fields, while the other techniques measure the velocity at a point.

A typical PIV apparatus consists of a camera (normally a digital camera), a strobe or laser with an optical arrangement to limit the physical region illuminated (normally a cylindrical lens to convert a light beam to a sheet), a synchronizer to act as an external trigger for control of the camera and laser, the seeding particles and the fluid under investigation. PIV software is used to post-processes the optical images.

Seeding particles

The seeding particles are a component of the PIV system. Depending on the fluid under investigation, the particles must be able to match the fluid properties reasonably well, otherwise they will not follow the flow satisfactorily enough for the PIV analysis to be considered accurate. Refractive index for the seeding particles should be different from the fluid which they are seeding, so that the laser sheet incident on the fluid flow will reflect off of the particles and be scattered towards the camera.

As for sizing, the particles should be small enough so that response time of the particles to the motion of the fluid is reasonably short to accurately follow the flow, yet large enough to scatter a significant quantity of the incident laser light. Due to the small size of the particles, the particles' motion is dominated by stokes drag and settling or rising effects. The particles are typically of a diameter on the order of 10 to 100 micrometers. The seeding mechanism needs to also be designed so as to seed the flow to a sufficient degree without overly disturbing the flow.

In the present experiments the fluid was seeded with clay, directly poured on the water in the flume. After some time for letting the system disperse properly the seeds, the particles reflected properly the incident laser sheet.

Figure 23. Clay for seeding the water

Camera

To perform PIV analysis on the flow, two exposures of laser light are required upon the camera from the flow. Fast digital cameras using CCD (charge-coupled device) chips can capture two frames at high speed with a few hundred ns difference between the frames. This has allowed each exposure to be isolated on its own frame for an accurate cross-correlation analysis. The limitation of typical cameras is that this fast speed is limited to a pair of shots. This is because each pair of shots must be transferred to the computer before another pair of shots can be taken. Typical cameras can only take a pair of shots at a much slower speed than the interval time between the two coupled frames.

Figure 24. Charge-Coupled Device (CCD) videocamera

Laser and optics

For macro PIV setups, lasers are predominant due to their ability to produce high-power light beams with short pulse durations. This yields short exposure times for each frame.

The optics consist of a spherical lens and cylindrical lens combination. The cylindrical lens expands the laser into a plane while the spherical lens compresses the plane into a thin sheet. This is critical as the PIV technique cannot generally measure motion normal to the laser sheet and so ideally this is eliminated by maintaining an entirely 2-dimensional laser sheet. It should be noted though that the spherical lens cannot compress the laser sheet into an actual 2-dimensional plane. The minimum thickness is on the order of the wavelength of the laser light and occurs at a finite distance from the optics setup (the focal point of the spherical lens). This is the ideal location to place the analysis area of the experiment.

The correct lens for the camera should also be selected to properly focus on and visualize the particles within the investigation area.

Figure 25. Laser head in position for the experiments

Synchronizer

The synchronizer acts as an external trigger for both the camera and the laser. Controlled by a computer, the synchronizer can dictate the timing of each frame of the CCD camera's sequence in conjunction with the firing of the laser to within 1 ns precision. Thus the time between each pulse of the laser and the placement of the laser shot in reference to the camera's timing can be accurately controlled. Knowledge of this timing is critical as it is needed to determine the velocity of the fluid in the PIV analysis.

Arrangement scheme (configuration)

The version of the Particle Image Velocimetry Software was 3.5 from TSI. This software is divided into two modules, an acquisition and a presentation module. The first acquires the PIV image and processes it to obtain the velocity vectors then automatically validates vector data, removes bad vectors and interpolates drop-out points. The presentation module calculates flow properties of vorticity and strain rates and displays the results as arrows and/or colours and contour levels.

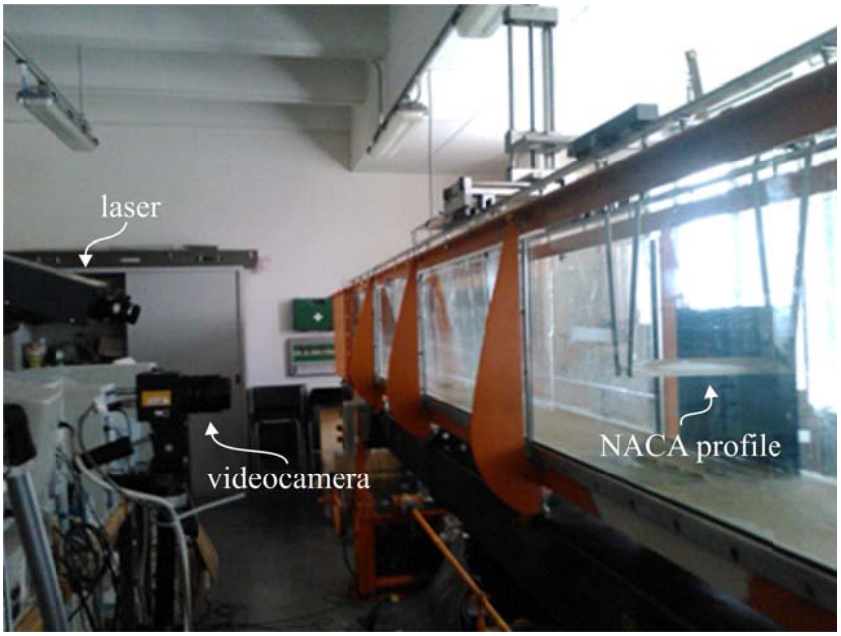

Figure 26. General view of the arrangement scheme

There were also two elements more in the arrangement scheme. The first was a mirror placed in the bottom of the flume, with the major size parallel to flow direction, in the centreline of the flume, and with its shortest dimension at 40° with the horizontal. The angle was evaluated according to reflection law and to Snell's law of refraction computing $\gamma = \cos^{-1}[(n_{H20}/n_{air}) \cos 2\alpha]$, where n_{H20} and n_{air} are the index of refraction for green light in water and in air respectively; the glass walls act only in translating the light sheet, being plane and of uniform thickness. Hence a limiting value of the argument of the sine function is requested: $[(n_{H20}/n_{air}) \cos 2\alpha] < 1$ or $\alpha > ½ \cos^{-1}(n_{air} / n_{H20})$. Assuming $n_{H20} = 1.33$ and $n_{air} = 1$ results $\alpha > 20° 40'$. In this way laser sheet could be reflected perpendicular to the bottom of the flume and is parallel to the centerline plane of the flume and lets the camera to record images in the plane of the light sheet. For $\alpha = 40°$ results $\gamma \approx 76°$. The thickness of the sheet layer experiences a minor reduction. The second element was a dark surface in the back glass side of the flume to let the image captured to be more clear. The front glass side of the flume and also the mirror placed in the bottom should be carefully cleaned with an anti-lime product.

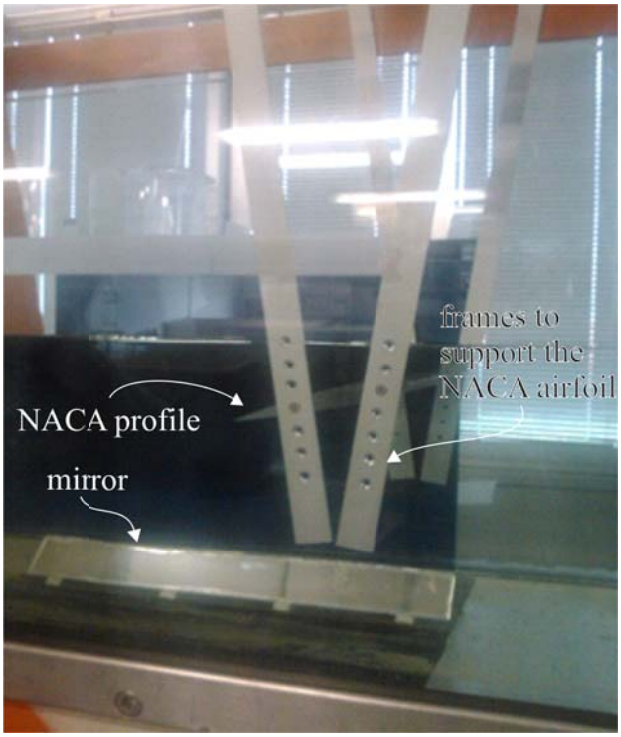

Figure 27. Layout of the mirror and the NACA airfoil (the inclination of the profile in the photograph is the opposite of the real one adopted in the tests)

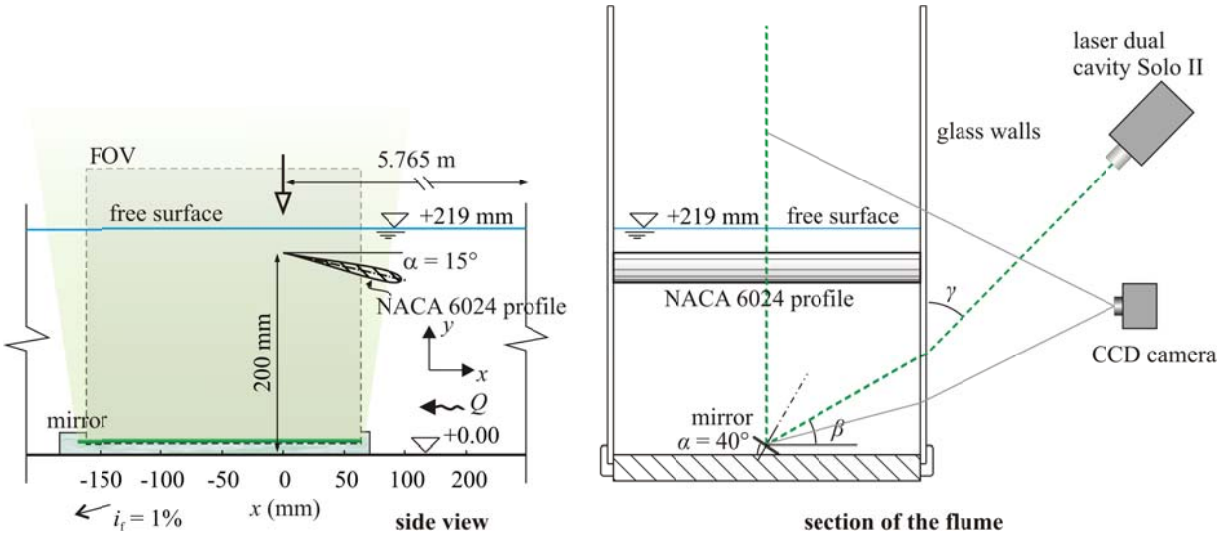

Figure 28. General layout of the experiments

Calibration of the PIV

To calibrate the PIV a grid was used in order to evaluate the transformation from pixels into coordinates and to refer properly the velocity vectors measured later. The mesh was suspended from above and in the same direction as the sheet illuminated with the beam reflected by the mirror and also recorded with the camera, as it can be seen in Figure 28.

The main steps to calibrate are the following. First to position the grid coincident to the reflected laser sheet and then fill the flume with the fluid (water). After waiting some time until the grid stabilizes and does not move, it is time to check that the grid and the camera base lines are horizontal, then focus the camera and store some images of the grid. Last step is to save the images. In this case, the images were saved in the folder for the experiments created in the disk.

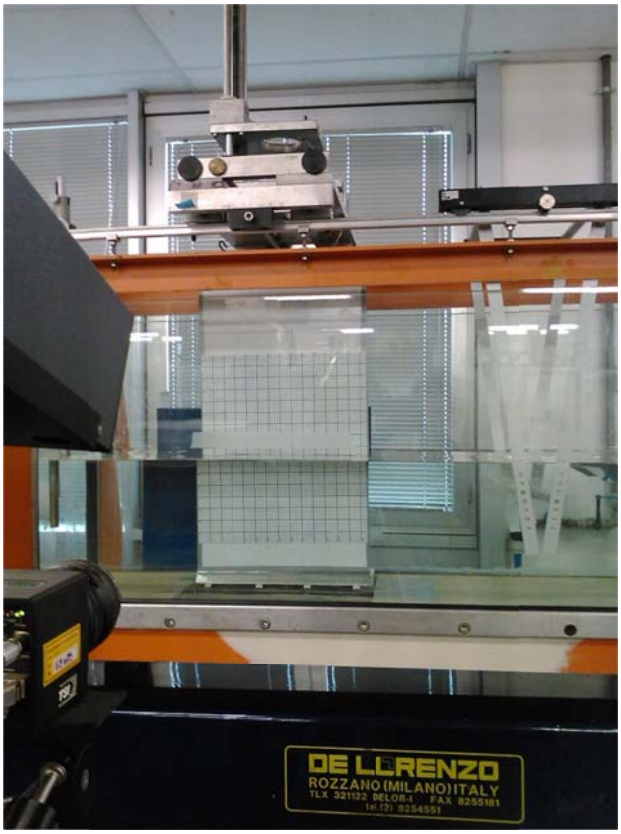

Figure 29. Calibration mesh suspended in the flume in the sheet light of the laser

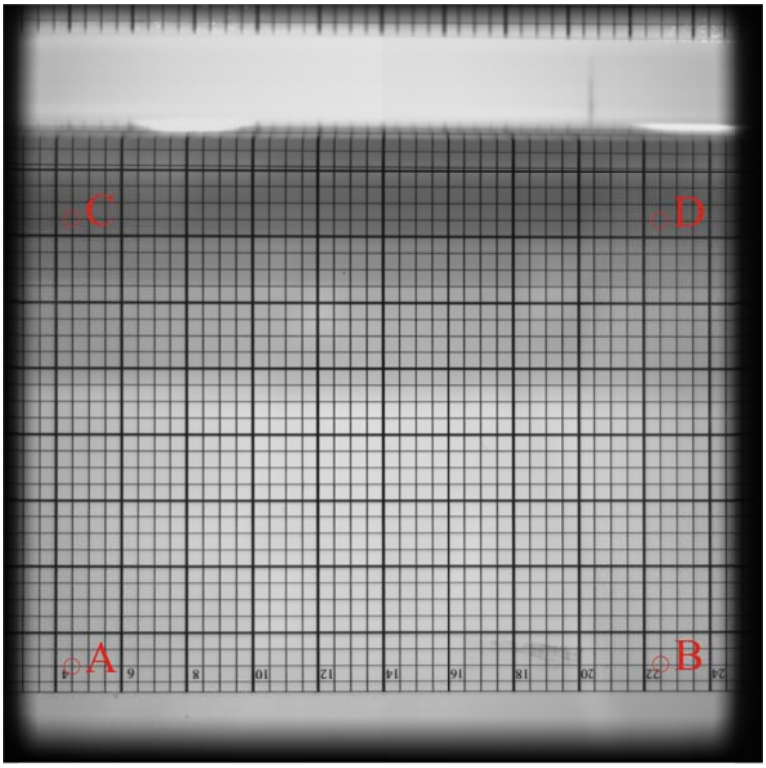

Figure 30. Calibration mesh suspended in the flume as video recorded by the videocamera

Quick tour to get results for an experiment

If something is not clear or a more detailed information is needed, please refer to the PIV System Operation Manual.

The first step is to specify and check hardware components, to check which hardware components are installed and to specify for them and then to check if they are all properly installed. From the Experiment menu, select Component Setup. The Component Setup dialog box appears and then perform the following steps:

- Click on the Summary tab and check to make sure that the values that appear in the Camera Model, the Laser Model, the Image Shifter (if using), the Synchronizer Model, and the Frame Grabber boxes are correctly specified and correspond to your system configuration. If not, go to the individual tabbed dialog boxes and make the appropriate changes. It is important that the hardware components in your system are part of the system configuration.
- Click on the Synchronizer Setup lab, check the Comm. Port that the Synchronizer is connected to, set all other values shown in the screen, and press Apply.
- Click on the Camera Setup tab in the Component Setup dialog box, use the settings for the camera used, select Synchronizer Triggered from the Timing Master group box, and press Apply.

- Click on the Laser Setup tab in the Component Setup dialog box, select the Model you are using, Enter a value of 15.0 in the Flashlamp Frequency box, Leave other settings at their default values, and press Apply.
- Click on the Computer-Controlled Camera Setup tab in the Component Setup dialog box, select Synchronizer Port B from the Camera Comm Port group box, leave other settings at their default values, and press Apply.
- Click on the I/O Board tab in the Component Setup dialog box, click the Enable box to start communication with the I/O board, select the voltage range for the analog input, select the Flumes, indicating where the analog inputs are connected, by checking the box next to the Flume Number, display analog data on the screen by using the Refresh Data button. The default output for the analog input is in voltage. However the voltage can be converted to physical units by using a 4^{th} order polynomial equation. Use the Map Flumes button to get to the Flume Map dialog. Enter the appropriate values for the coefficients, K, A, B, C, and D. It is assumed that you will supply the coefficients. Hence calibration to establish the conversion factor is needed. The INSIGHT software does not perform any calibration to relate the analog inputs to their physical units. The analog data is captured at the same time with the PIV images.
- Click on the Summary tab and check to make sure that the information that appears in the Camera Model, the Laser Model, the Image Shifter (if using), the Synchronizer Model, and the Frame Grabber boxes is still correct, then press OK. Make sure that the messages: Synchronizer Ready and Camera Ready appear in the Status bar. If they do not appear, make sure the Comm Port settings for the camera are set correctly by performing Step E again. Sometimes it also helps to turn off and then turn on the Synchronizer to reset and accept all the new settings and values.

Second step is to create a new experiment.

- To create a new experiment folder choose New from the Experiment menu, then the New dialog box appears. Specify a name for your experiment. INSIGHT stores all experiment data files in the specified folder under the Experiments folder that is created during installation. It also creates three additional folders: Calibration, Image, Vector for each experiment.
- To Setup the Experiment specify the following values for the parameters in the Capture Dialog Bar:
  Data Source: Camera
  Exposure Mode: Frame Straddle
  Capture Mode: Continuous
  In the Timing Dialog Bar, click on the clock (Timing Parameters) icon and specify a value in μs for the d*T* (pulse separation) parameter. Then press Apply and Close.
  In the Laser dialog box, click on the YAG power levels icon and specify the values for Pulse Energy Selection for YAG1 and YAG2. In the Laser dialog box set energy levels for both lasers. Choose Save from the Experiment menu.

To Open an Experiment File just choose Open from the Experiment menu, the Open dialog box appears, and specify the path and filename for the experiment file.

To Acquire PIV Images.

- Click on the camera (Begin Image Acquisition) icon on the main menu bar. Make sure the images are being captured. The images are displayed continuously. If no images appear after a period of time, a warning message “Acquisition Timeout” appears. Click on Frame A and then on Frame B

tabs on top of the images; make sure images appear on both frames. If they do not, the Pulse Delay value needs to change. Refer to the PIV Reference manual for details on how to calculate the appropriate pulse delay value. If the image acquisition sequence is proceeding continuously, press the STOP (Stop Operation) icon on the main menu bar to stop the image acquisition.

To Process Images and Display Vectors. It means to define or select an interrogation area and to process the image and to display vectors, the steps are the ones that follow.

- Select the Area of Interest icon from the Process menu, the cursor changes to a cross-hatch. Position the cursor in the upper left boundary of the region to be processed. Click and while holding the left-mouse button, drag the cursor down the bottom of the region for processing, this selects the area of interest. Click on the Begin Image processing icon to start processing. Observe the images and the vectors as they are being processed. In the following steps, you will be fine-tuning the processing. Select Setup from the Process menu, click on the Grid Setup tab, change the values of the parameters to the ones that better fit to the experiment. Press Apply and then close the dialog box.
  Select Area of Interest icon from the Process menu. The cursor changes to a cross-hatch. Position the cursor in the upper left boundary of the region to be processed. Click and while holding the left-mouse button, drag the cursor down the bottom of the region for processing. Click on the Begin Image Processing icon. Observe the images and the vectors as they are being processed.

To Validate the Vectors, to check if the generated vectors are valid.

- Choose Interactive Validation from the Vector menu. Check the Mean filter, and press Validate button to validate the vector field. Repeat using the Range button (the vector field is revised and displayed with each filter selection) Press Done, to get out of the validation dialog.

To Store the Data do Disk (once the vectors are validated, the images and the vectors for this capture can be stored in the Experiment directory).

- Select the Save Experiment and Image Fields icon from the System Control Tool Bar. Images are stored in the image subdirectory of the Experiments directory in the format of X00000a.tif and X00000b.tif (for two frames) where X is the Experiment name specified when the Experiment was created. Vectors are stored in the Vectors subdirectory in the format of X00001.vec where X is the Experiment name specified when the Experiment was created.

To Acquire a Sequence of Images to Computer RAM.

- From the Vector menu bar select Clear to clear the screen of any vectors generated in the previous step. From the Process menu bar select Sequence Scope / All. Select Sequence for the Capture Mode value in the Capture Dialog Bar, the Sequence Setup box appears. Enter a value in the Number of Captures box. Make sure there is sufficient storage in computer's RAM. An error message appears if the computer does not have adequate memory. Enter a value of 0 in the Start Number box. Select Save to RAM. Press Apply and then Close.
  Click on the Begin Image Acquisition icon in the System control Tool bar. The Specified number of captures is displayed in the Captures in Memory box that appears under the tool bar. Use the "play" control on the player panel to look at each image. Use the "advance" control on the player

panel to go through the sequence. Click on the Frame A or Frame B to check the image pair. Using the control buttons go back to Frame 00000.

To Process Sequences of Images. To use the sequence of images acquired in the previous step, and process them in a single batch for time-resolved data.

- From the Process menu, select Sequence Scope / All. From the Process menu again or the System Control Tool Bar select Area of Interest icon. The cursor changes to a double-headed arrow in a box. Position the cursor in the upper-left boundary of the image. Click and while holding the left-mouse button, drag the cursor down to the bottom of the image. Click on Begin Image Processing icon in the System Control Tool Bar. Vectors are generated for all the captures in the sequence specified.

Results

The following lines and figures show the results of the first test done with the PIV and the airfoil in the flume. The difference between this test and the ones in the appendix is the inclination of the airfoil (15° in Experiment 0 and 19°30' in Experiments 1-2-3) and the calibration (after Experiment 0 the system was moved and another calibration was needed, that was the definitive calibration for Experiments 1-2-3).

From now on this will be called Experiment 0 and was performed for a flow rate of 10 L/s

Position 1

Experiments performed on 07/07/2011

The first part of the first experiment was performed with the general scheme that can be seen in Figure 29.

The elements of the scheme are:

- The airfoil has an inclination of 15° (measured respect to the chord) with the horizontal.

- The adhesive tape mark, to reference every experiment to the first. It is also useful for the second position of the experiment.

- The rule in the upper part of the flume that measures the distance from the origin (upstream end of the flume).

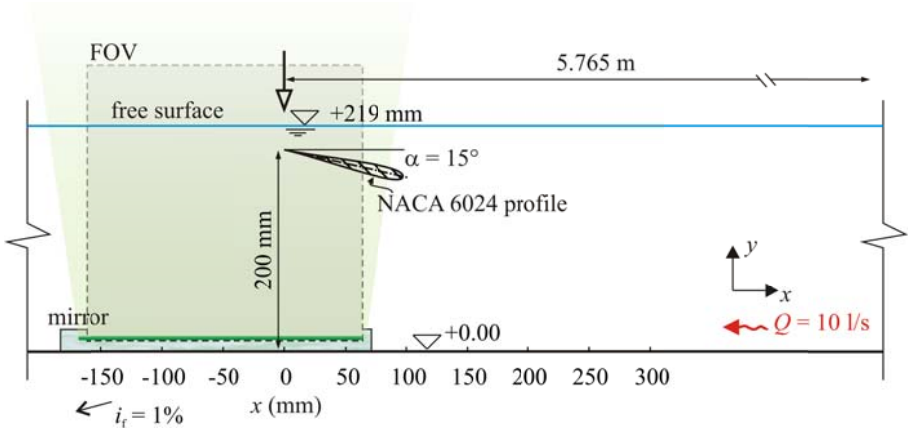

Figure 31. Layout for Experiment 0, Position 1

After switching on the pump at 11:10 a.m. it was necessary to wait 10 minutes to let the flow stabilize. Because any minor movement of the PIV or the CDD camera requires recalibration, the option of moving the airfoil upstream was considered and applied. In that way another FOV could be recorded with the PIV, and overlapped to the first obtained a larger area of measurements. The upstream movement of the airfoil induces a minor error, due to a different water level, but it negligible. The airfoil is moved upstream 150 mm and in some tests four different positions where analysed, obtaining a measurements area larger than 600 mm.

Position 2

Experiments performed on 08/07/2011

The disposition was similar to the one of the Position 1 but the airfoil was moved upstream 0.15 m. The layout is shown in Figure 32.

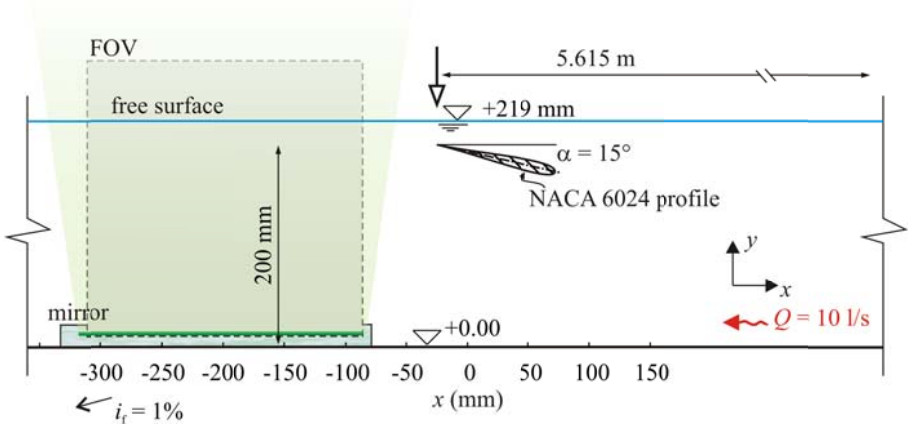

Figure 32. Layout for Experiment 0, Position 2

The database for Experiment 0 is reported in Table 2.

The root for the archives of this test is test_1_wing_wake***. Calibration was made using images stored in the pen drive and transferred to calibration folder. The criterion was validating data larger than the mean plus 1 standard deviation. Also some pictures were taken with videocamera and called still_image_test_1_wing_wake***

VOF	Q (m^3/s)	water temperature (°C)	frequency of acquisition (Hz)	dT (µs)	Number of frames	Local time	water depth (m)	position (rule) (m)	trailing edge elevation (m)	file name
1	10	-	3.00	2000	1000	-	0.219	5.765	0.200	test_1_wing_wake
2	10	23.12	3.00	2000	1000	11:55	0.219	5.615	0.200	test_2_wing_wake

Table 2. Experiment 0, database. Kinematic viscosity $\nu = 9.0969 \times 10^{-7}$ m^2/s, $U_\infty = -0.152$ m/s, Re = 16 700

The following figures report the results of postprocessing the data obtained with the PIV for Experiment 0, by overlapping the FOVs for Position 1 and Position 2.

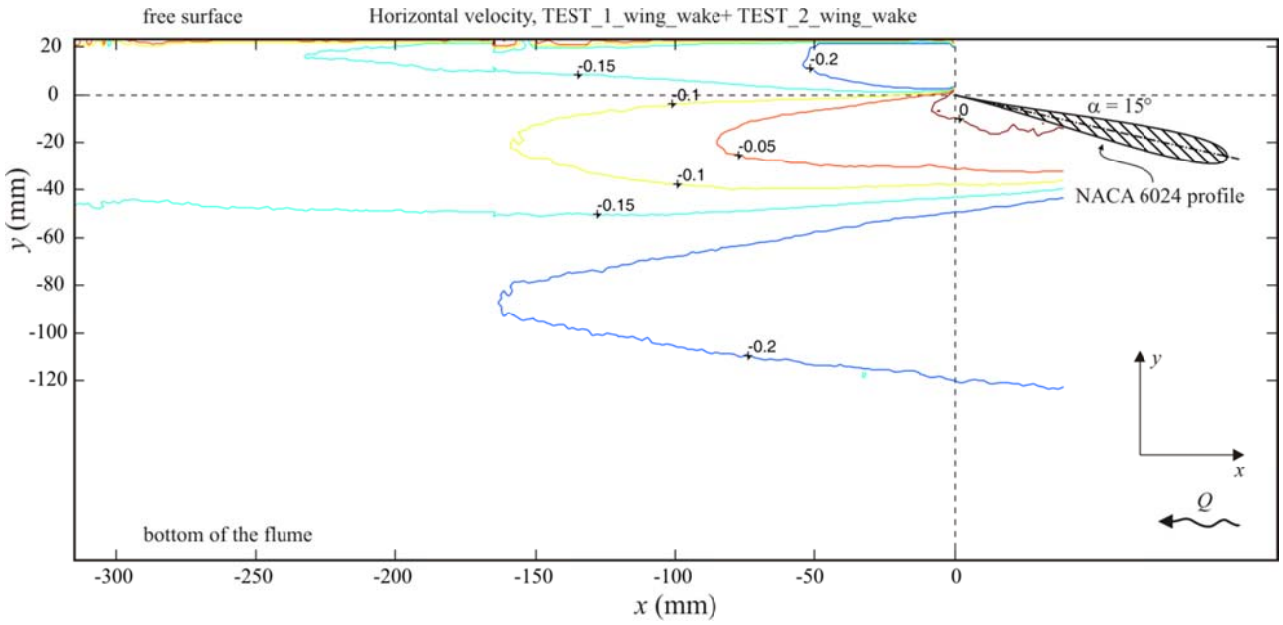

Figure 33. Experiment 0, mean horizontal velocity U (m/s). Q = 10 l/s, $U_\infty = -0.152$ m/s, 1000 frames, f_{acq} = 3 Hz

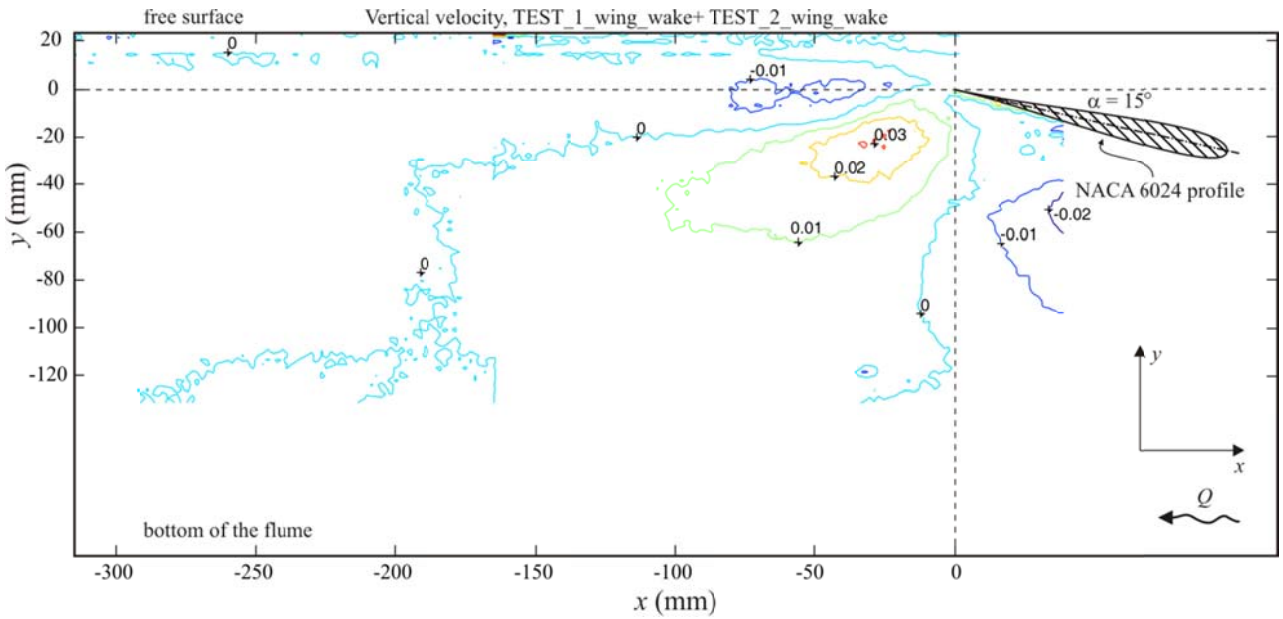

Figure 34. Experiment 0, mean vertical velocity V (m/s). Q = 10 l/s, U_∞= – 0.152 m/s, 1000 frames, f_{acq} = 3 Hz

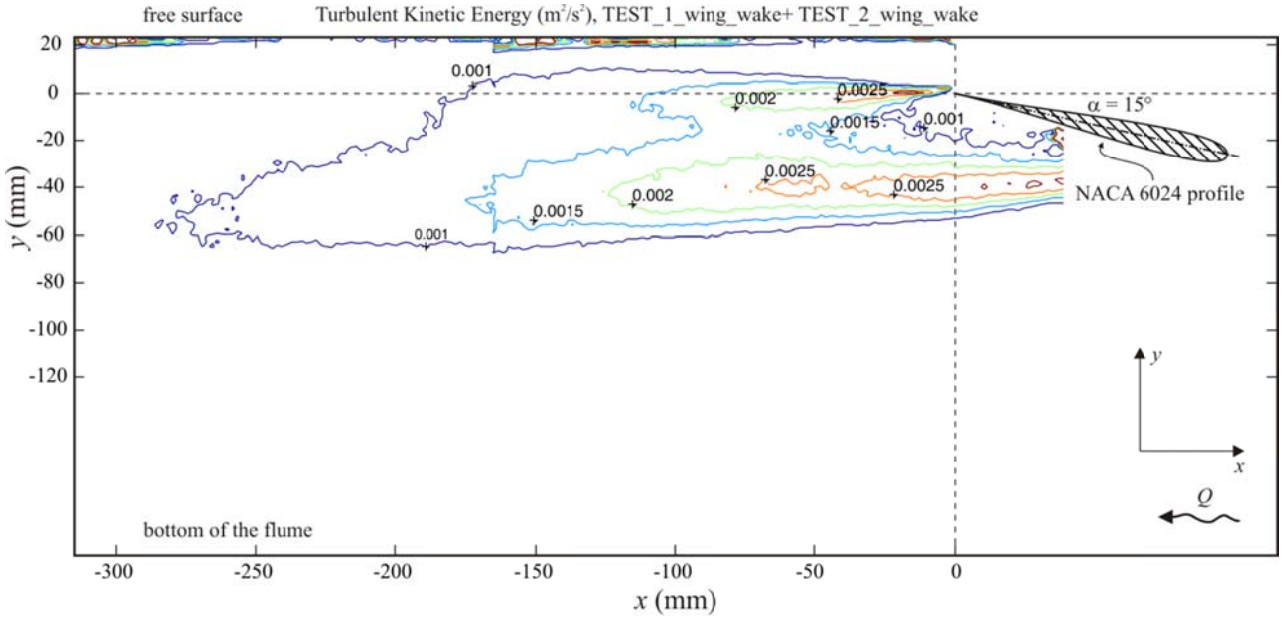

Figure 35. Experiment 0, Turbulent Kinetic Energy (TKE), (m^2/s^2). Q = 10 l/s, U_∞= – 0.152 m/s, 1000 frames, f_{acq} = 3 Hz

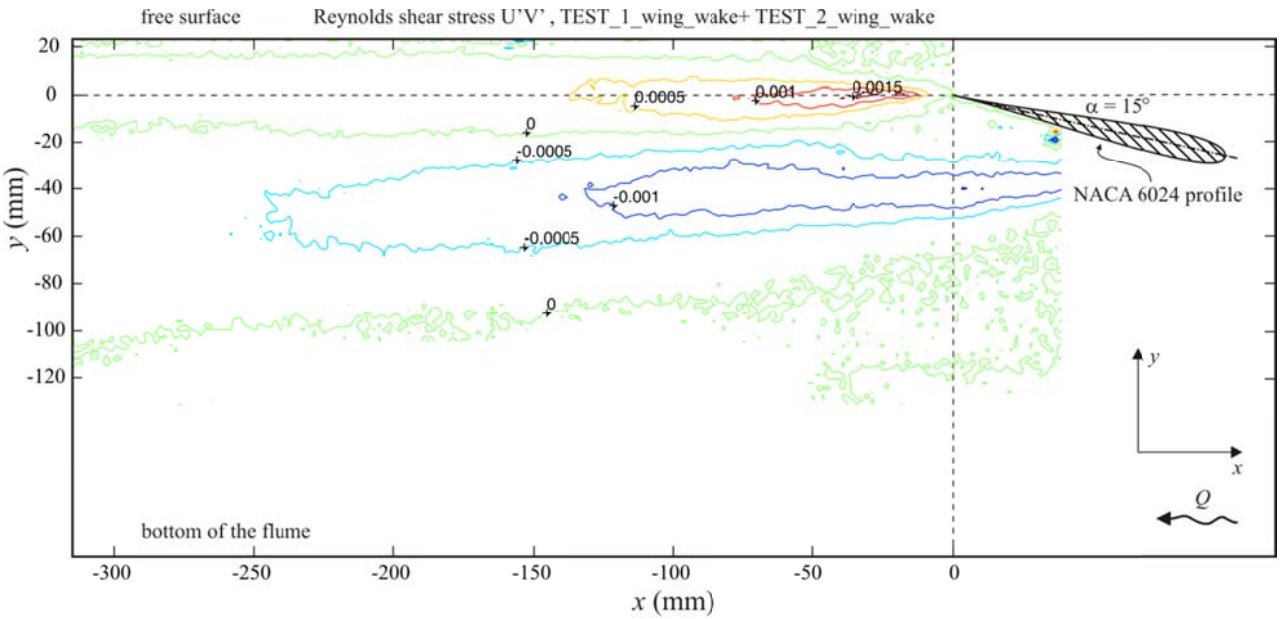

Figure 36. Experiment 0, Reynolds shear stress (m^2/s^2). Q = 10 l/s, U_∞= – 0.152 m/s, 1000 frames, f_{acq} = 3 Hz

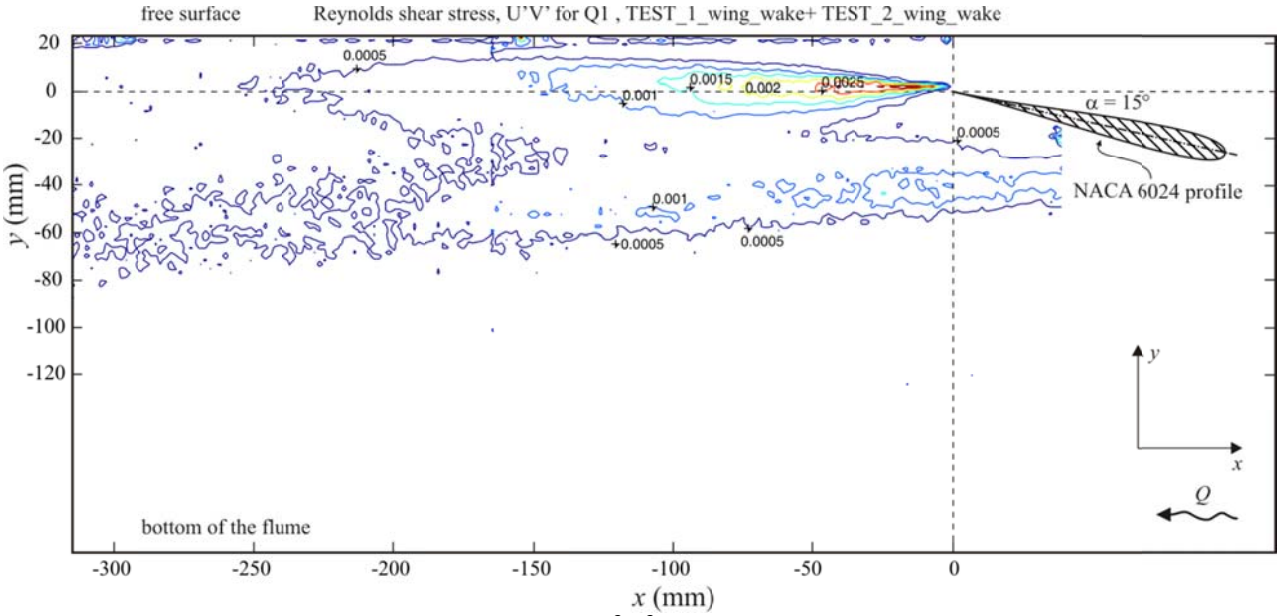

Figure 37. Experiment 0, Reynolds shear stress (m^2/s^2), quadrant Q1 (+U', +V'), phasic average. Q = 10 l/s, U_∞= – 0.152 m/s, 1000 frames, f_{acq} = 3 Hz

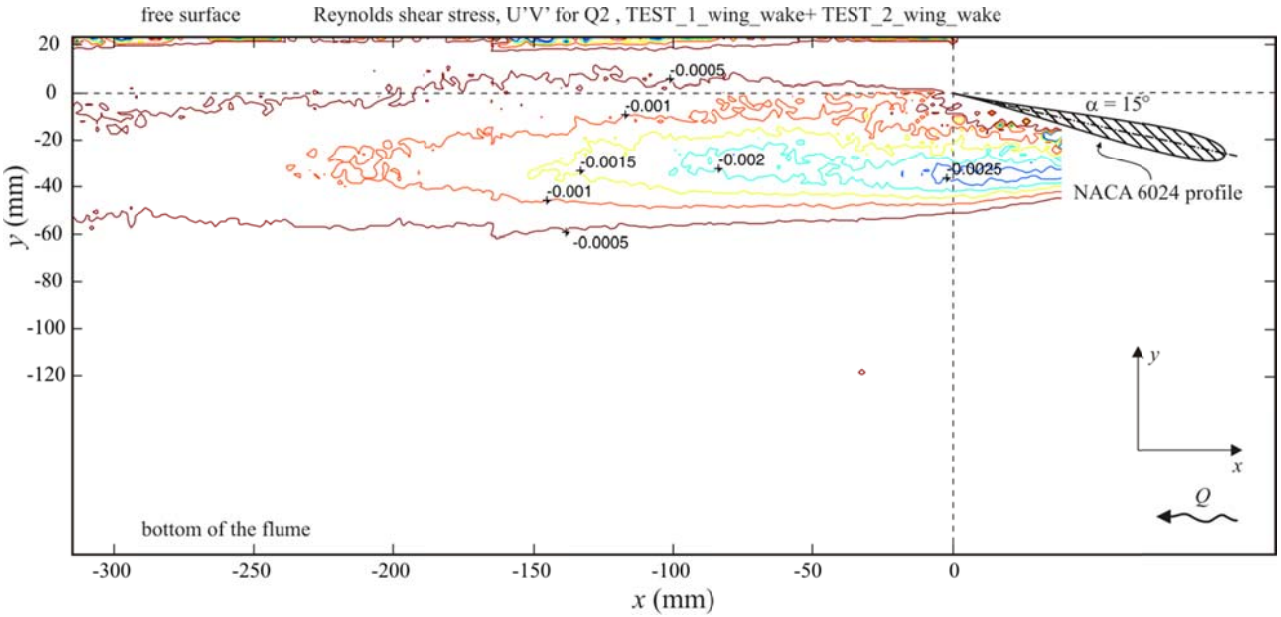

Figure 38. Experiment 0, Reynolds shear stress (m^2/s^2), quadrant Q2 ($-U'$, $+V'$), phasic average. Q = 10 l/s, U_∞= – 0.152 m/s, 1000 frames, f_{acq} = 3 Hz

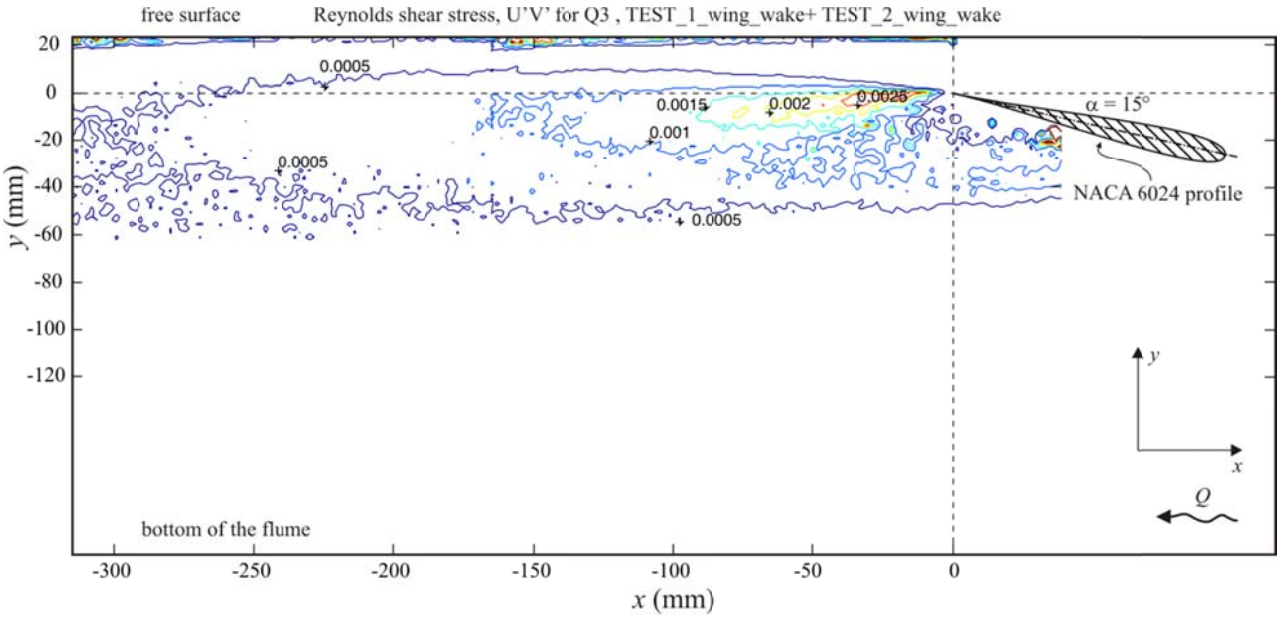

Figure 39. Experiment 0, Reynolds shear stress (m^2/s^2), quadrant Q3 ($-U'$, $-V'$), phasic average. Q = 10 l/s, U_∞ = – 0.152 m/s, 1000 frames, f_{acq} = 3 Hz

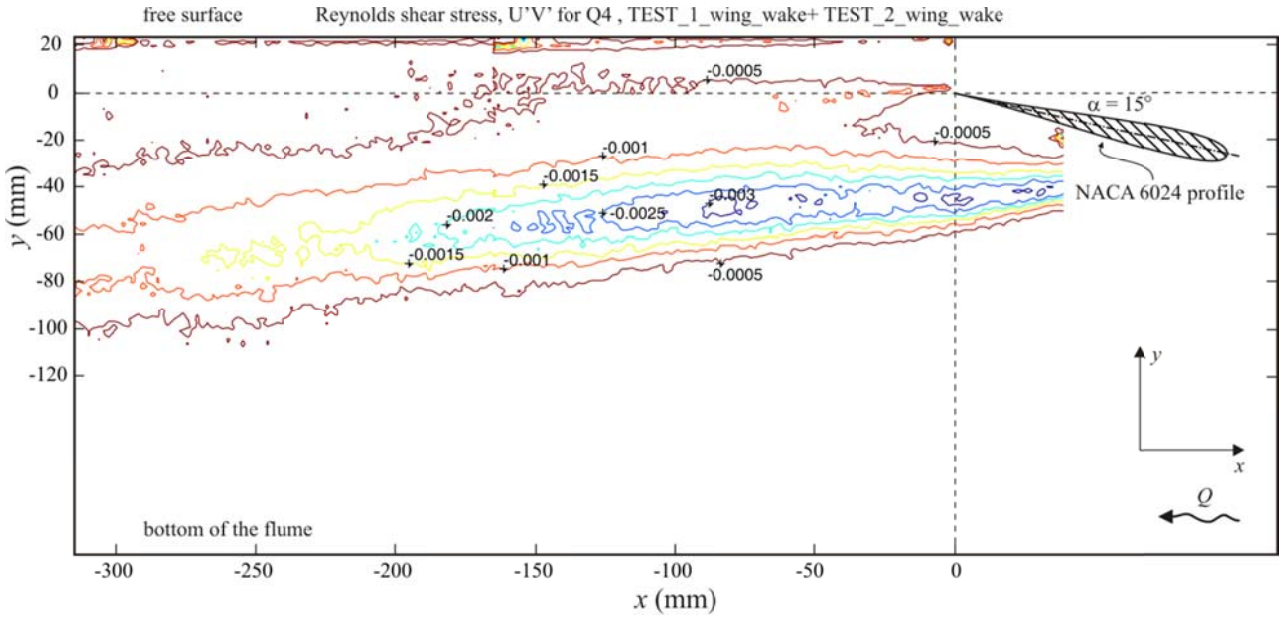

Figure 40. Experiment 0, Reynolds shear stress (m^2/s^2), quadrant Q4 ($+U'$, $-V'$), phasic average. Q = 10 l/s, U_∞ = – 0.152 m/s, 1000 frames, f_{acq} = 3 Hz

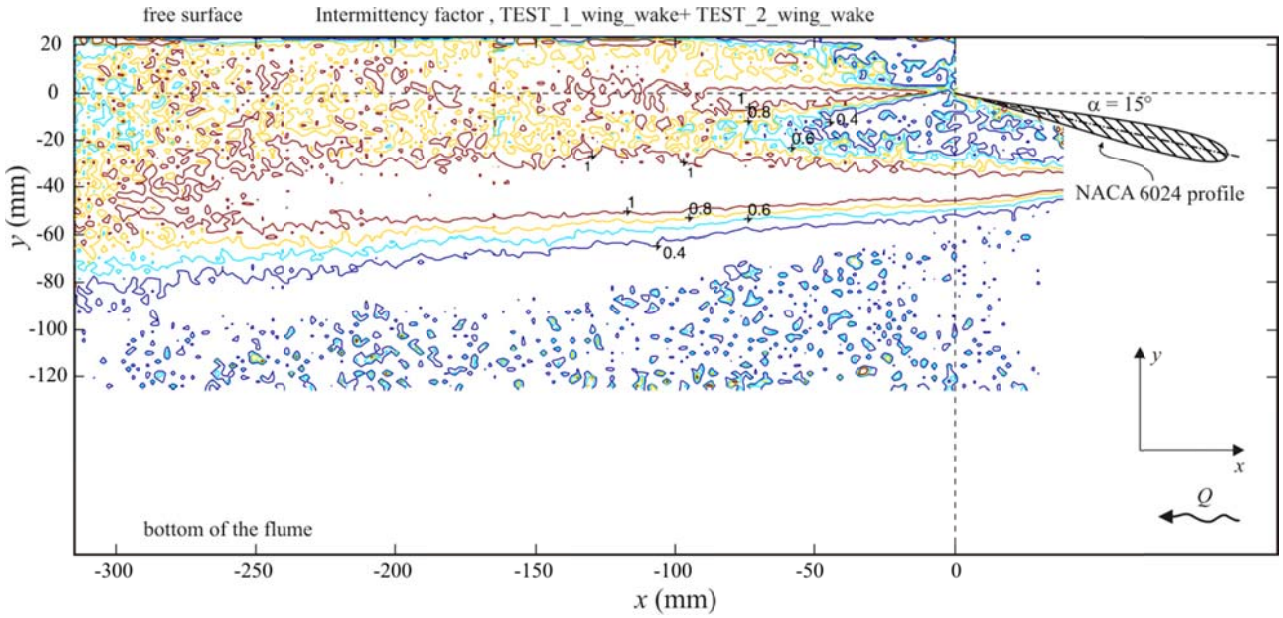

Figure 41. Experiment 0, Intermittency factor. Q = 10 l/s, U_∞ = – 0.152 m/s, 1000 frames, f_{acq} = 3 Hz

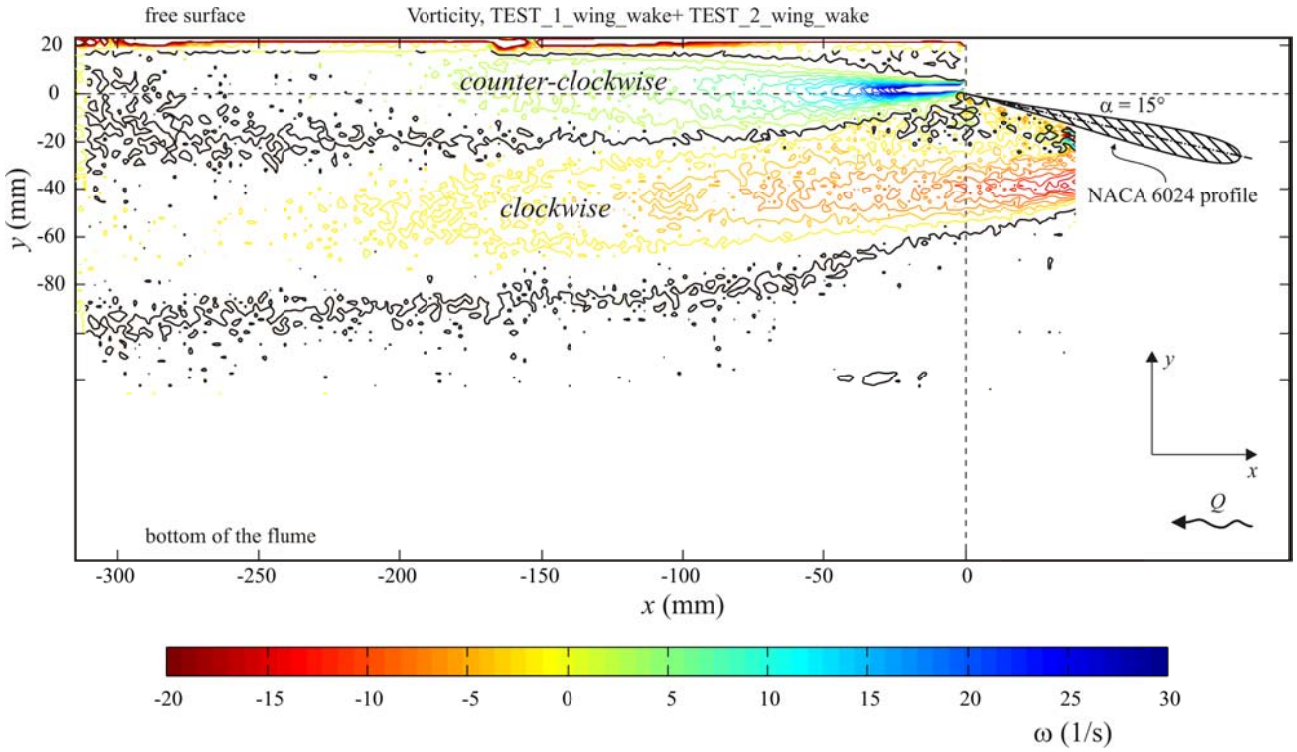

Figure 42. Experiment 0, Vorticity. Bold black line is the zero vorticity isoline. Q = 10 l/s, U_∞ = – 0.152 m/s, 1000 frames, f_{acq} = 3 Hz

ULTRASONIC SENSOR FOR DISTANCE MEASUREMENTS

Water level oscillations were measured by an ultrasonic water level sensor (US), model Q45UR, produced by the company Turck-Banner, see Figure 43.

Figure 43. Ultrasonic water level gauge

The sensor consists of a piezoelectric transducer immersed in an alternate electrical field, whose voltage oscillates at a certain frequency; the transducer responds to the electric excitation, vibrating at a high frequency and emitting an ultrasonic pressure wave burst. The ultrasonic wave packet propagates in air towards the water free surface, where it is reflected. This reflected wave packet travels back to the sensor,

where it is collected by the same membrane that emits the wave. The sensor measures the time elapsed between the emission of the ultrasonic pulse and the reception of the reflected pulse and hence determines the distance (d) from the membrane to the target through the relation:

$d = ½ c t_f$

where t_f is the flight time of the ultrasonic wave and c is the celerity of the ultrasonic wave in air. Since c is a function of temperature, the sensor s equipped with a temperature gauge to compensate for the effects of temperature variations.

Calibration of the ultrasonic sensor

The voltage output of the ultrasonic sensor must be related to a metric water level signal. The input – output relation (mm – V) is determined by measuring a number of known distances; to do so, the water level is kept still and the gauge is moved to known locations by means of a traverse system. For each location, the output signal is acquired for a time interval in seconds, the mean voltage value is then computed and associated with the known distance from the water surface. The long-range calibration curve is plotted and also the short-range calibration curve, and used to translate the voltage measurements, taken in the experiment, into distances.

Disposition of the ultrasonic sensor

The US was placed in the flume suspended from above to measure the evolution of the level of the water free surface.

To adjust the sensing distance the steps are the following:

- Hold push button for approximate 2 seconds until green LED turns off.
- First limit (near or far) Place target at first limit and click push button less than 2 seconds.
- Second limit* (near o far) Place target at second limit and click push button less than 2 seconds.

*Target positions must be at least 5 mm apart. If the target is held at the same position a 5mm range sensing window is established centered around the object.

The measurements taken with the ultrasonic sensor have not yet been analysed.

3. REFERENCES

Battjes J.A., Sakai T., (1981), Velocity field in a steady breaker. J. Fluid Mech., vol. 111, pp. 421-437.

Chiapponi L., Longo S., Bramato S., Mans C., Losada M.A., (2011), Waves generated by wind Experiments carried out in wind tunnel II CEAMA, Granada, Spain, July 2010. Technical Report

Jacobs E.A., Ward K.E., Pinkerton R.M. (1933), The Characteristics of 78 Related Airfoil Sections from Tests in the Variable-Density Wind Tunnel, Report No. 460, National Advisory Committee for Aeronautics, Navy Building, Washington D.C.

Particle Image Velocimetry (PIV) System. Operations Manual. TIS Incorporated

Peregrine D.H., Svendsen I.A. (1978) Spilling breakers, Bores and hydraulic jumps, Proc. 16th Int. Conf. Coastal Eng., Vol 1 (1978), pp. 540–550

4. APPENDIX 1

Details of the experiments

Experiment 1

Experiment 1 was performed with a flow rate of 15 L/s

First part

First part of the first experiment was performed with the general scheme that can be seen in Figure 43.

The elements of the scheme are:

- The airfoil, that has an inclination of 19°30' with the horizontal.
- The adhesive tape mark, to reference the exact position of the airfoil, also useful to the second and/or third positions of every experiment (explained below).
- The rule in the upper part of the flume that measures the distance from the origin (upstream head of the flume)

Figure A1. Rule in the upper part of the flume

Figure A2. Picture of the layout, Experiment 1, Position 1

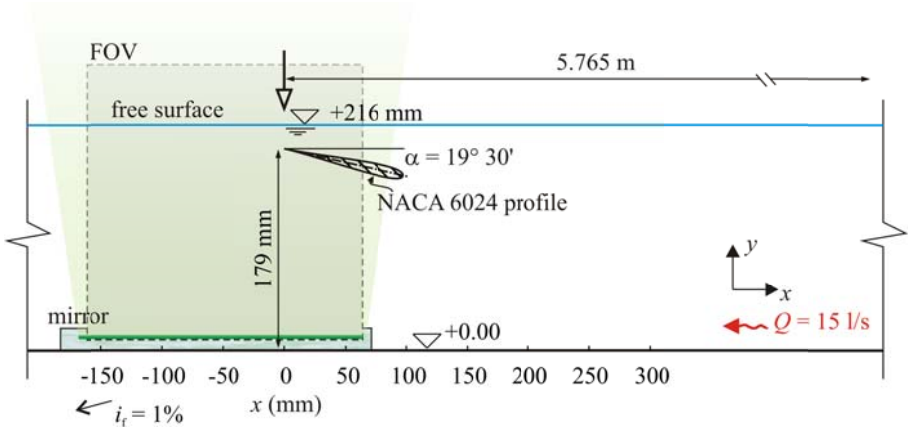

Figure A3. General layout for Experiment 1, Position 1

Because any minor movement of the PIV or the camera requires recalibration, the option of moving the airfoil upstream was considered. In that way a new FOV could be recorded with the PIV, to join to the first and get a larger area of measurements. In Experiment 1 three different positions of the airfoil where analysed, the second one with the airfoil position 0.15 m upstream, the third one with the airfoil position 0.30 m upstream respect to the first one. The rest of the layout was identical to the one of the Position 1.

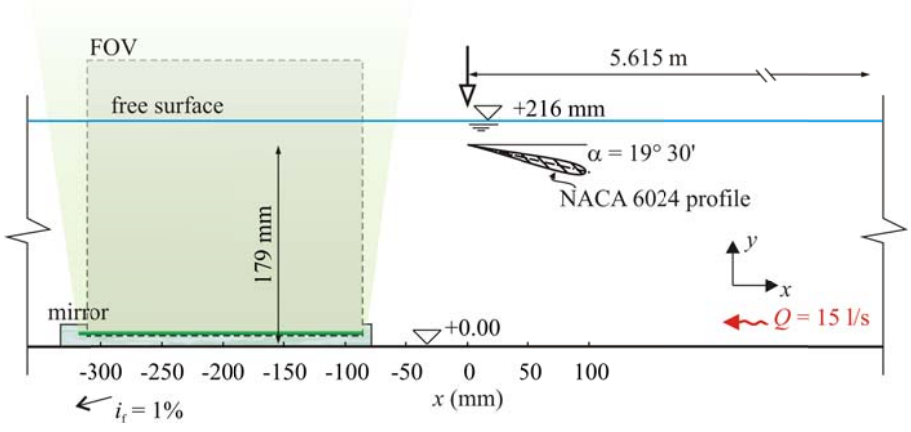

Figure A4. General layout for Experiment 1, Position 2

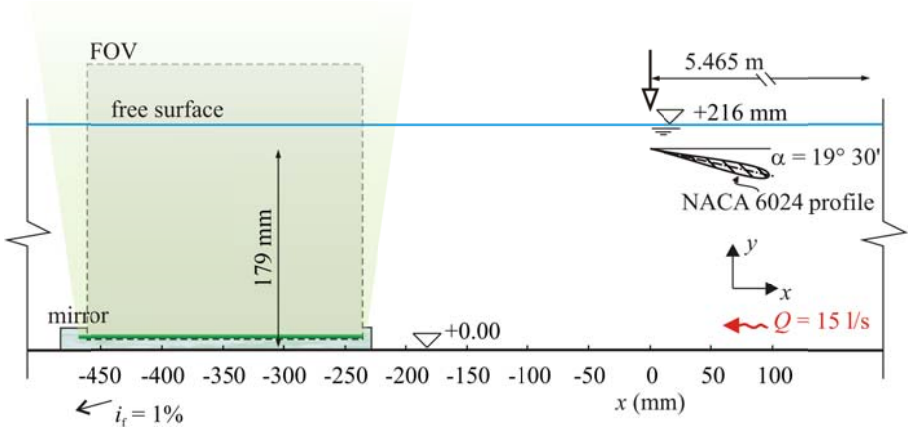

Figure A5. General layout for Experiment 1, Position 3

The data base for Experiment 1 is synthesized in Table 3.

VOF	Q (m^3/s)	water temperature (°C)	frequency of acquisition (Hz)	dT (μs)	Number of frames	Local time	water depth (m)	position (rule) (m)	trailing edge elevation (m)	file name
1	15	22.67	3.75	2000	1000	17:49	0.216	5.765	0.179	test_3_wing_wake
2	15	23.54	3.75	2000	1000	18:12	0.216	5.615	0.179	test_4_wing_wake
3	15	23.94	3.75	2000	1000	18:35	0.216	5.465	0.179	test_5_wing_wake

Table 3. Data base for Experiment 1.

Kinematic viscosity $\nu = 9.1926 \times 10^{-7}$ m^2/s, $U_\infty = -0.23$ m/s, Re = 25 100

Experiment 2

In Experiment 2 the flow rate is equal to 20 L/s, with 4 different positions of the airfoil. Due to the higher flow rate, compared to Experiment 1, it can be seen in Figure A6 that the free surface perturbations are much more evident.

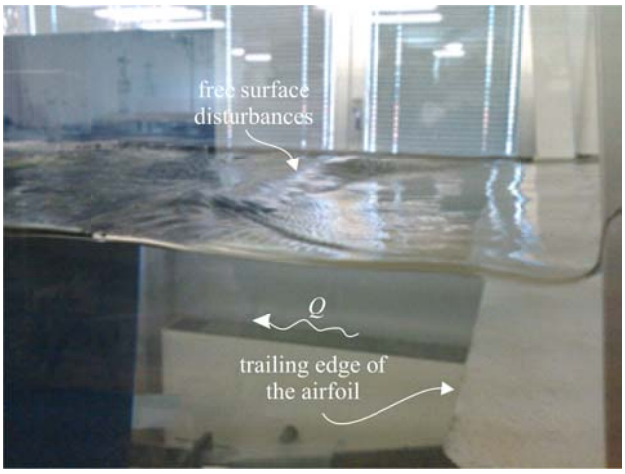

Figure A6. Water surface near the airfoil, Experiment 2 (20 L/s)

The general layout for the four positions in Experiment 2 is shown. Respect to Experiment 2 a fourth position has been added since the disturbances are larger hence more persistent in the flume.

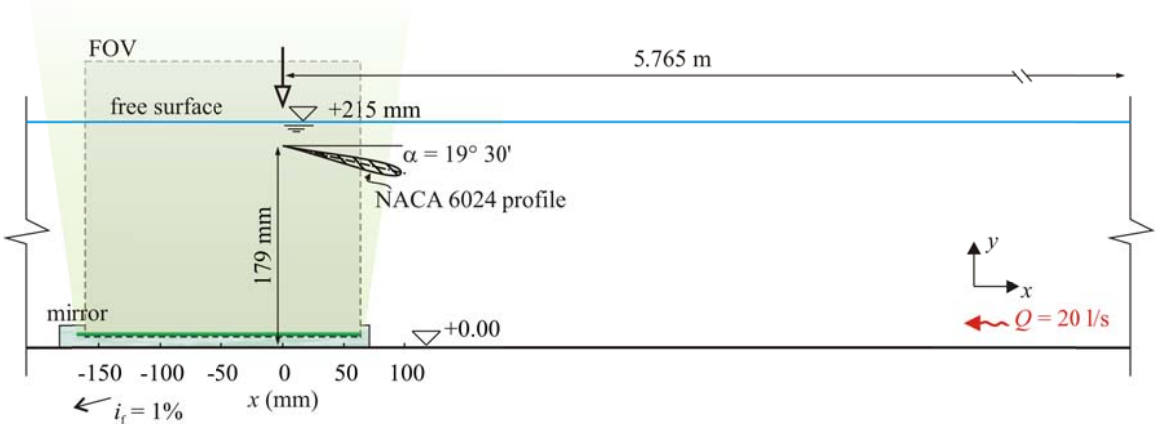

Figure A7. Layout for Experiment 2, Position 1

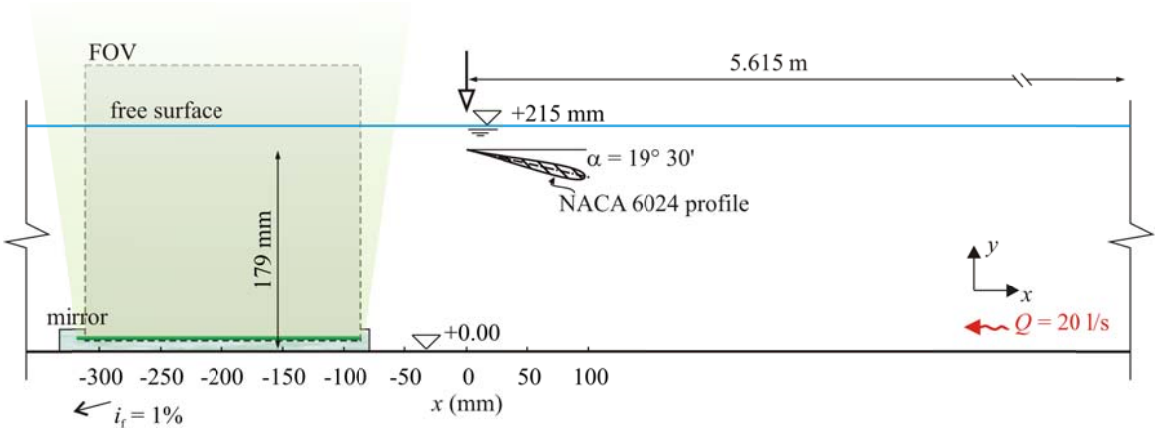

Figure A8. Layout for Experiment 2, Position 2

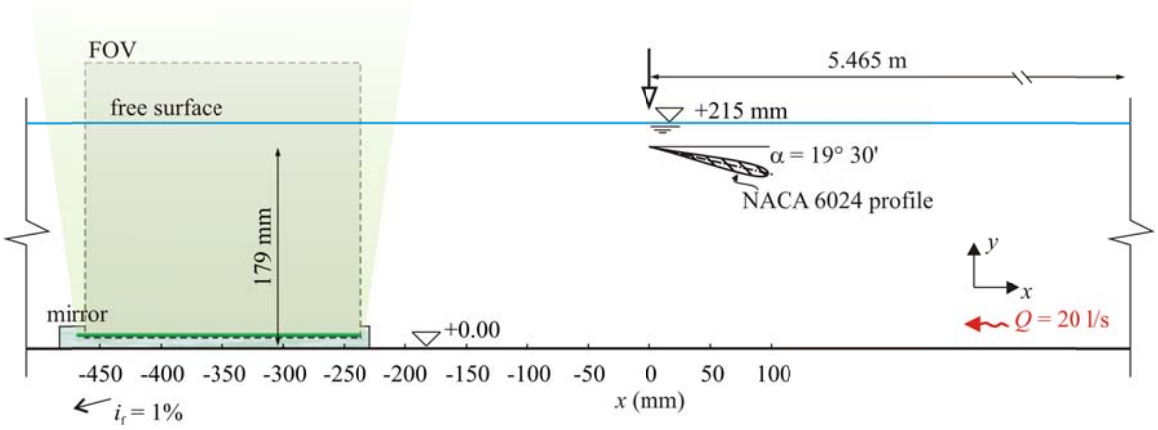

Figure A9. Layout for Experiment 2, Position 3

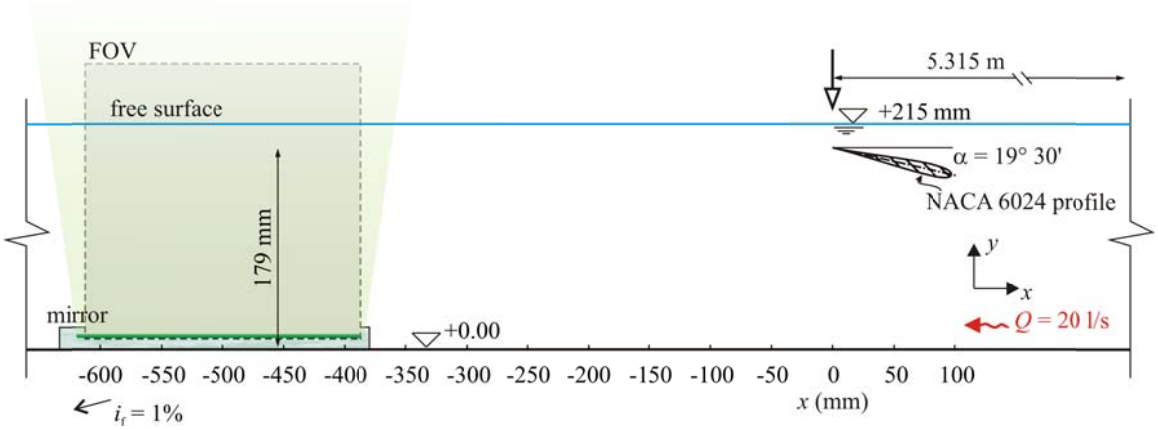

Figure A10. Layout for Experiment 2, Position 4

The data base of Experiment 2 is reported in Table 4.

VOF	Q (m^3/s)	water temperature (°C)	frequency of acquisition (Hz)	dT (μs)	Number of frames	Local time	water depth (m)	position (rule) (m)	trailing edge elevation (m)	file name
1	20	24.94	3.75	2000	1000	16:02	0.215	5.765	0.179	test_6_wing_wake
2	20	25.70	3.75	2000	1000	16:30	0.215	5.615	0.179	test_7_wing_wake
3	20	26.04	3.75	2000	1000	16:52	0.215	5.465	0.179	test_8_wing_wake
4	20	26.32	3.75	2000	1000	17:15	0.215	5.315	0.179	test_9_wing_wake

Table 4. Main characteristics of every part of the Experiment 2.

Kinematic viscosity $\nu = 8.7256 \times 10^{-7}$ m^2/s, $U_\infty = -0.31$ m/s, Re = 35 500

Experiment 3

Experiment 3 was performed following the same steps as for Experiment 2 but with a flow rate of 25 l/s. Due to the higher flow rate, compared to first and second experiments, the free surface shows more evident fluctuations, see Figure A11. A jump is evident.

Figure A11. Water surface in Experiment 3 (25 L/s)

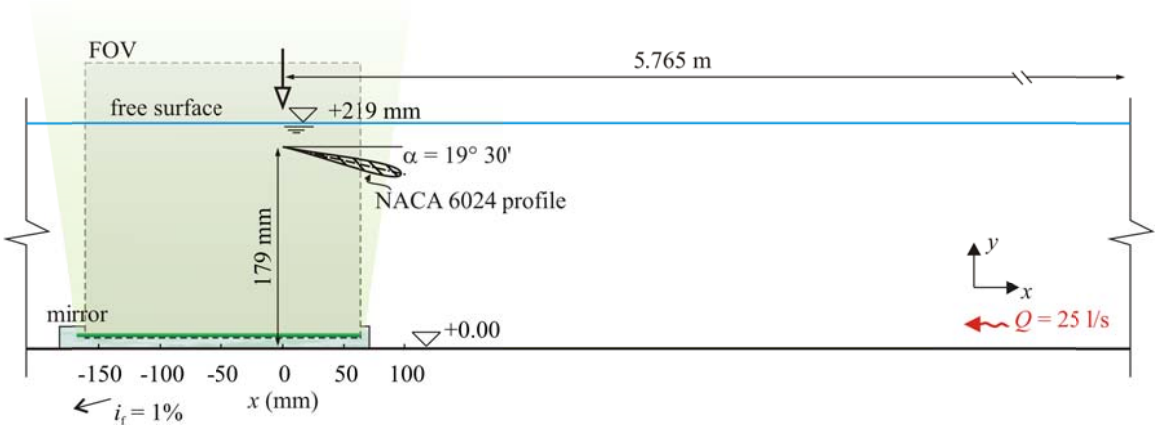

Figure A12. Layout for Experiment 3, Position 1

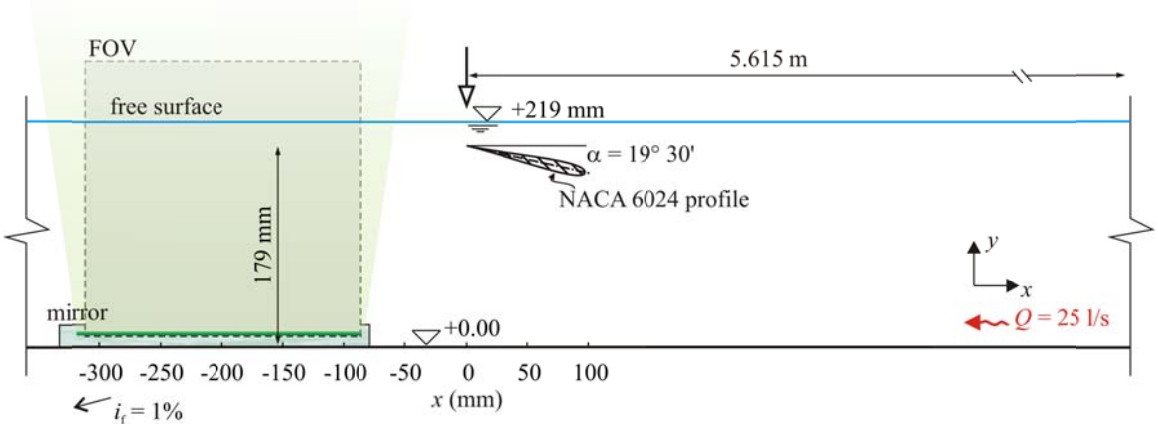

Figure A13. Layout for Experiment 3, Position 2

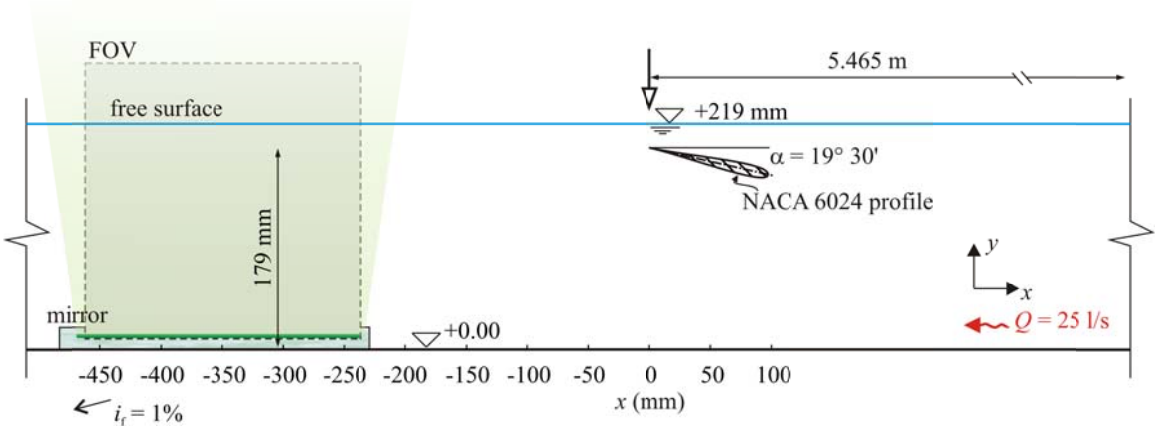

Figure A14. Layout for Experiment 3, Position 3

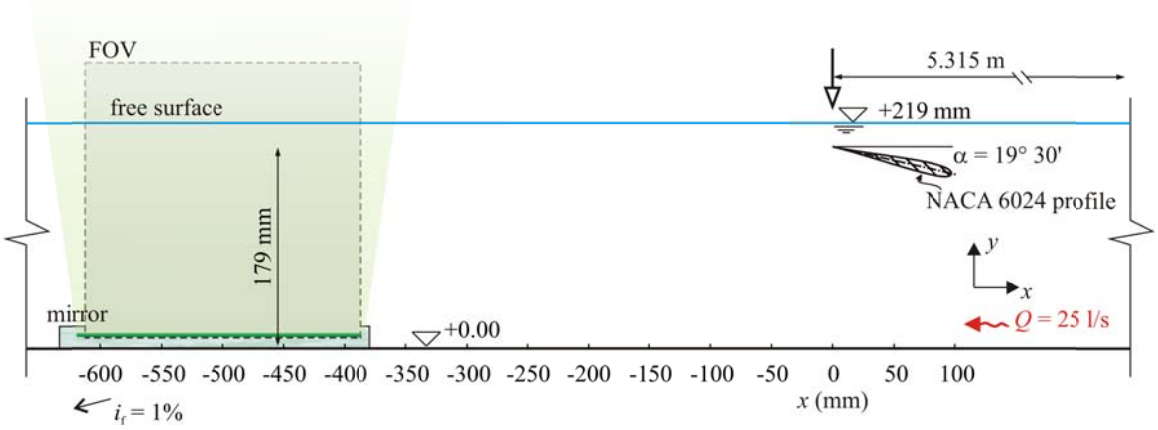

Figure A15. Layout for Experiment 3, Position 4

The data base for Experiment 3 is reported in Table 5.

VOF	Q (m^3/s)	water temperature (°C)	frequency of acquisition (Hz)	dT (μs)	Number of frames	Local time	water depth (m)	position (rule) (m)	trailing edge elevation (m)	file name
1	25	27.00	3.75	2000	1000	18:06	0.219	5.765	0.179	test_10_wing_wake
2	25	27.36	3.75	2000	1000	18:33	0.219	5.615	0.179	test_11_wing_wake
3	25	27.68	3.75	2000	1000	18:55	0.219	5.465	0.179	test_12_wing_wake
4	25	27.90	3.75	2000	1000	19:15	0.219	5.315	0.179	test_13_wing_wake

Table 5. Database for Experiment 3

Kinematic viscosity $\nu = 8.3334 \times 10^{-7}$ m^2/s, $U_\infty = -0.38$ m/s, Re = 45 700

5. APPENDIX 2

Coordinates of the airfoil

To determine the coordinates of the entire airfoil the following Matlab routine was developed.

```
clear all
close all
clc
%NACA 6024
c=1; %in m
delta=0.024; %in m
t=(24/100)*c; %thickness

x1=[0.000001:0.000002:0.001];
m=6; % maximum camber of 6% (in tenths of the cord) located at the
airfoil leading edge (0%)
p=0;

for i=1:length(x1)
    yc1(i)=(m/(1-p)^2)*((1-2*p)+2*p*x1(i)-x1(i)^2);
    yt1(i)=(t/0.2)*(0.2969*sqrt(x1(i))-0.1260*x1(i)-
0.3516*(x1(i)^2)+0.2843*x1(i)^3-0.1015*(x1(i)^4));
    theta1(i)=atan((m/p^2)*(2*p-2*x1(i)));
    xu1(i)=x1(i)-yt1(i)*sin(theta1(i));
    yu1(i)=yc1(i)+yt1(i)*cos(theta1(i));
    xl1(i)=x1(i)+yt1(i)*sin(theta1(i));
    yl1(i)=yc1(i)-yt1(i)*cos(theta1(i));
end

x2=[0.001:0.004:c];

for j=1:length(x2)
    yc2(j)=(m/(1-p)^2)*((1-2*p)+2*p*x2(j)-x2(j)^2);
    yt2(j)=(t/0.2)*(0.2969*sqrt(x2(j))-0.1260*x2(j)-
0.3516*(x2(j)^2)+0.2843*x2(j)^3-0.1015*(x2(j)^4));
    theta2(j)=atan((m/p^2)*(2*p-2*x2(j)));
    xu2(j)=x2(j)-yt2(j)*sin(theta2(j));
    yu2(j)=yc2(j)+yt2(j)*cos(theta2(j));
    xl2(j)=x2(j)+yt2(j)*sin(theta2(j));
    yl2(j)=yc2(j)-yt2(j)*cos(theta2(j));
end

x=[x1 x2];
yc=[yc1 yc2];
yt=[yt1 yt2];
theta=[theta1 theta2];
xu=[xu1 xu2];
yu=[yu1 yu2];
```

```
xl=[xl1 xl2];
yl=[yl1 yl2];

plot(x,xu)
hold on
plot(x,xl)
save('NACA4Spormi', 'xu', 'yu', 'xl', 'yl', 'x', 'yc')
```

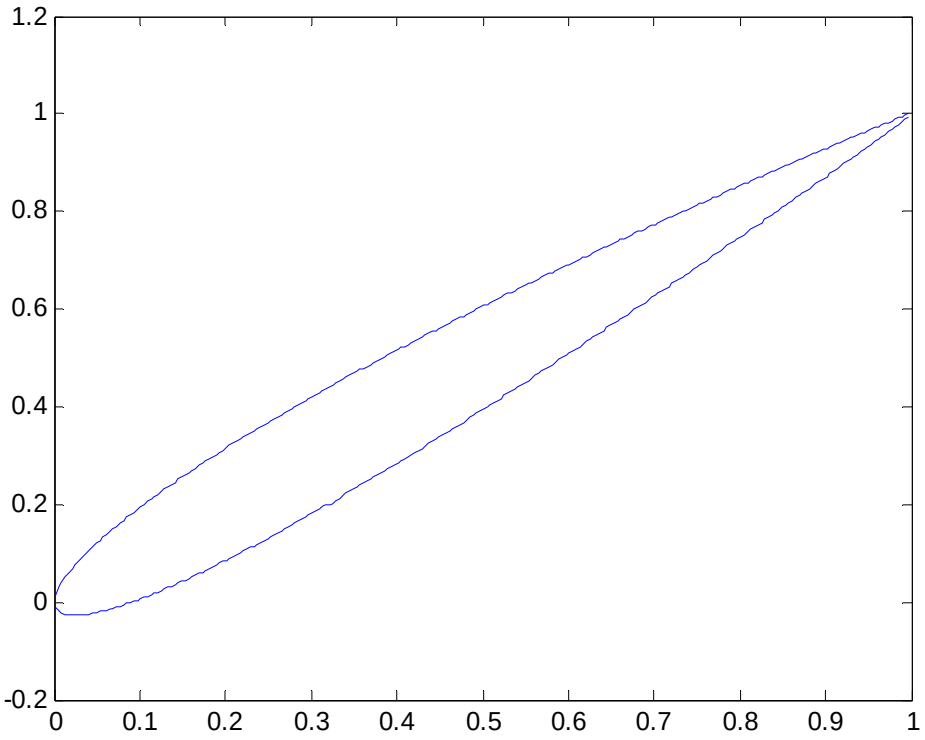

Figure A16. Section of the airfoil

The archive NCA4Spormi was imported in AutoCad and plotted in 3D to give the exact coordinates to the miller company that finally made the airfoil in Polymethyl methacrylate.

6. APPENDIX 3

Getting data with the UDVP

Using this matlab routines velocity profiles in axis “x”, “y” and “z” could be got, and also kinetic energy and turbulence.

First step is to create the compatible file with the data from the doppler, using following short routine that calles the functions below:

```
% 16/05/2011 (Parma) Francisco Manuel Dominguez Luque

clear all

close all

clc


[vel,echo,z,t]=BinDop('Fran130611_15-8.bdd',6000);


save('Resultado32.mat', 'vel', 'echo', 'z', 't') ;
```

```
function [prof1,prof2,Pos,timestamp,tgc,mpxflume,par,mpxpar]=BinDop(file,num);
function [VDop,FDop]=dopplerfreq(par,prof1);
function tgc=gain(par,fid,B4OS,Pos);
function [I,Q]=IandQ(B2OS,B5OS,fid);
function mpxpar=multiplexer(fid,mpxflume,B3OS);
function [timestamp,prof1,prof2,mpxflume]=profiles(par,fid,B5OS,num,numflume);
```

The archives with these functions will be attached in the same folder as this Project.

Once the archive is made and the variables “echo” and “velocity” extracted as individual archives, it can be used following routine to get velocity profiles, kinetic energy and turbulence.

```
%Francisco M. Dominguez Luque (18/05/11) Parma

clear all

close all
```

```
clc

%Charging Velocity and Echo archives

%BINDOP.M with the archives recorded with UDV in multiplexer mode.

load Velocity.mat;

load Echo.mat;

%Note that 3000 is for the example made. It is the number of profiles recorded and it should be changed if different.

v1=[1:3:3000];

v2=[2:3:3000];

v3=[3:3:3000];

echo1=echo(:,v1);

echo2=echo(:,v2);

echo3=echo(:,v3);

vel1=vel(:,v1);

vel2=vel(:,v2);

vel3=vel(:,v3);

nn=length(echo1(1,:));

mm=length(echo1(:,1));

vector=(1:1:nn);

corrvelx=[];

corrvely=[];

corrvelz=[];

th=(75*2*pi)/360; %in rad

be=(30*2*pi)/360;
```

```
% B is the change of axis matrix
A=[-cos(th) sin(th) 0; cos(th)*sin(be) sin(th) cos(th)*cos(be);
   cos(th)*sin(be) sin(th) -cos(th)*cos(be)];
B=inv(A);

%Velocity for each axis x y z
velocx=vel1*B(1,1)+vel2*B(1,2)+vel3*B(1,3);
velocy=vel1*B(2,1)+vel2*B(2,2)+vel3*B(2,3);
velocz=vel1*B(3,1)+vel2*B(3,2)+vel3*B(3,3);

%Right velocity values are gotten, by substituing NaN in each value that corresponds to an echo
value grater than a saturation value.

for i=1:nn
 ecu1(:,1)=echo1(:,[i]);
 velox(:,1)=velocx(:,[i]);
 veloy(:,1)=velocy(:,[i]);
 veloz(:,1)=velocz(:,[i]);

 io=find(ecu1(20:mm)<0);
 if io>0
    none=ecu1(io(1,1)+19:mm)*NaN;
    velox(io(1,1)+19:mm)=none;
    veloy(io(1,1)+19:mm)=none;
    veloz(io(1,1)+19:mm)=none;

    corrvelx=[corrvelx velox];
    corrvely=[corrvely veloy];
    corrvelz=[corrvelz veloz];
```

```
 end
end

%Calculamos la concentracion de NaN's que hay en cada fila
UXI=[];
for j=1:mm
   UXI=[UXI; isnan(corrvelx([j],:))];
   media(j)=mean(UXI([j],:));
   concentracion(j,1)=1-media(j);
end
    save('ResultadoX.mat', 'corrvelx') ;
 figure(1), hold on
plot(mean(corrvelx'))
figure(2), hold on
plot(mean(corrvely'))
figure(3), hold on
plot(mean(corrvelz'))
figure(4), hold on
plot(concentracion)
%Turbulent component of the velocity
longitud=length(corrvelx(1,:));
corrturbx=corrvelx-repmat(nanmean(corrvelx'),longitud,1)';
corrturby=corrvely-repmat(nanmean(corrvely'),longitud,1)';
corrturbz=corrvelz-repmat(nanmean(corrvelz'),longitud,1)';
%plot(nanstd(corrturbx'))
%Kinetic energy
k=1/2*(nanstd(corrturbx').^2+nanstd(corrturby').^2+nanstd(corrturbz').^2);
figure(5), hold on
plot(k)
```

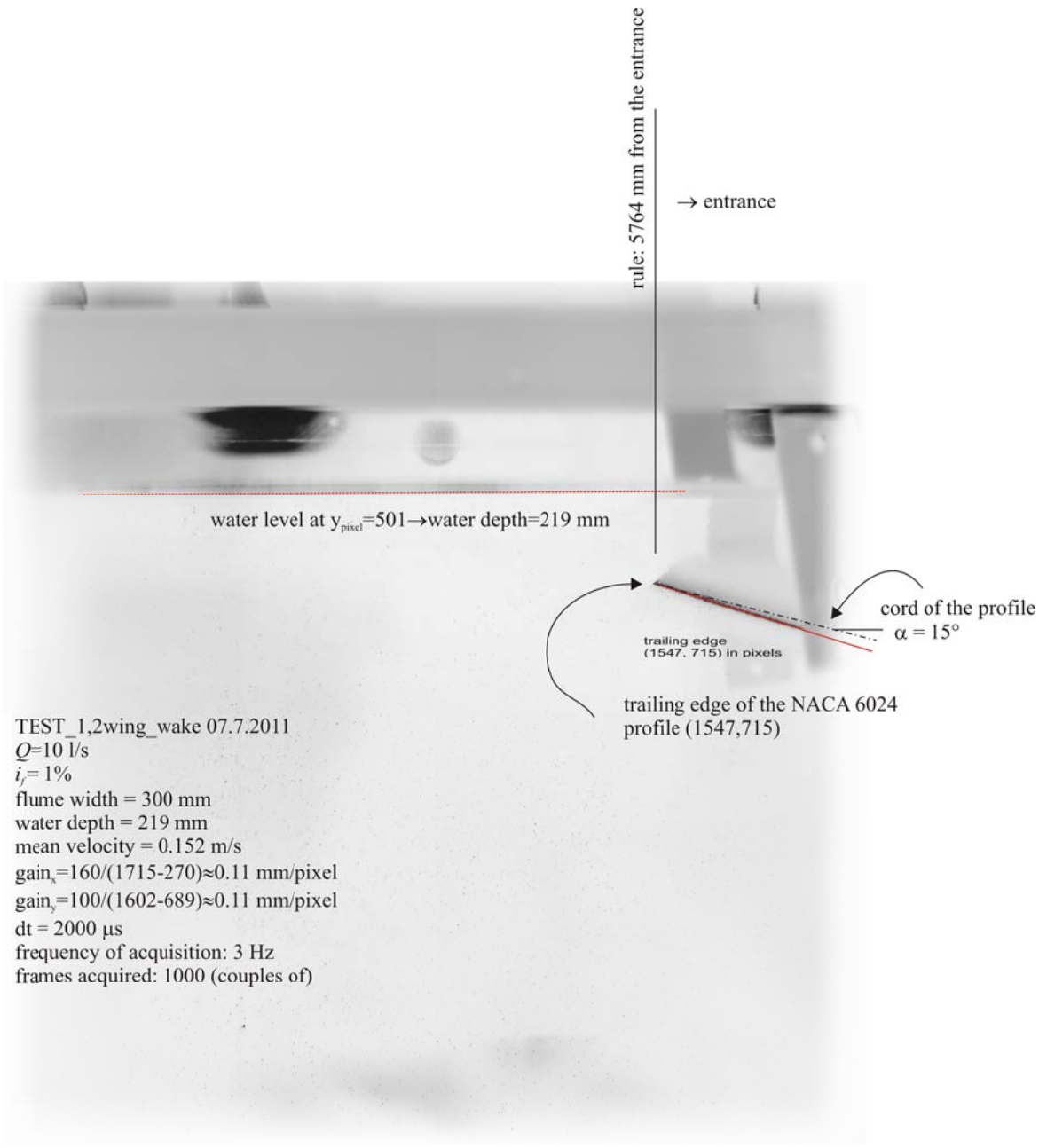

Figure A17. Data for calibrating PIV data, test_1 and test_2

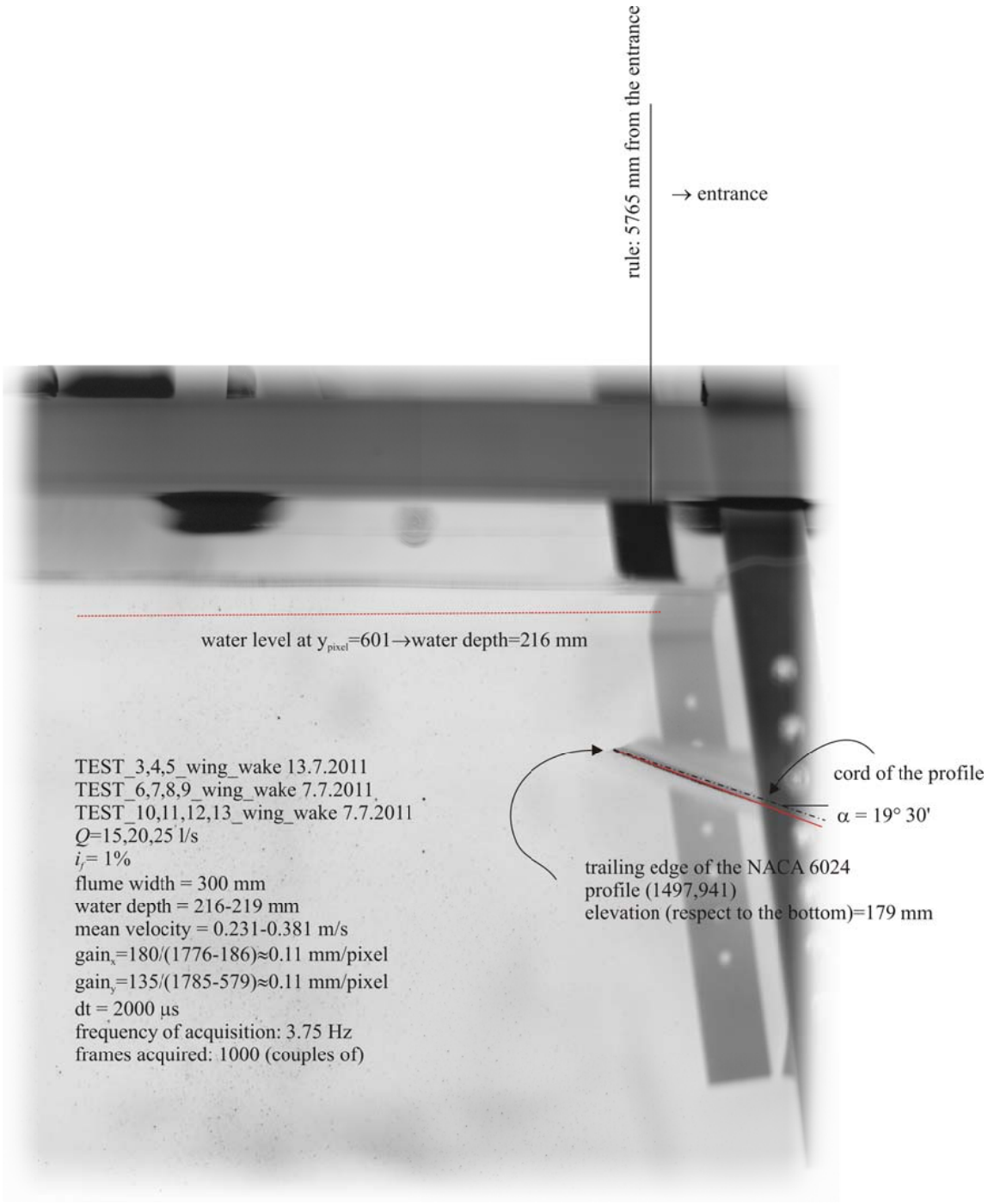

Figure A18. Data for calibrating PIV data, test_3-test_13